Expression, Purification and Crystallisation Studies with the M_2 Muscarinic and H_1 Histamine Receptors.

Amanda Aloia
BSc. in Nanotechnology (Honours)

A thesis submitted for the degree of Doctor of Philosophy in
Biology.

School of Biological Sciences
Faculty of Science and Engineering
Flinders University, South Australia

April 2008

The writing of this thesis.

Image courtesy of Ms Rebecca Attwood, CSIRO MHT, Parkville.

Destruction of small rainforest (also called "editing")

Piles of lab books

Concentrated caffeine

Unfit, under rested, stressed…but still smiling! (most of the time ☺)

Free food from generous, sympathetic tea-lady

Overworked computer

Constant reminder of time left

Jumper from location of Post-Doc (motivational tool)

Overworked computer

Unprocessed data from last minute experiments

Thesis writing was powered by:
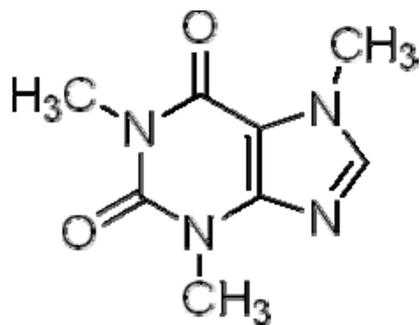
This thesis is tree-friendly!

In an effort to repair the environmental destruction caused by the production of this thesis a donation was made to the Carbon Neutral Program – www.carbonneutral.com.au.

This donation will be used to plant 50 new trees which will process 7.6 tonnes of CO_2.

Financial Support

This thesis, and the work within, was gratefully financially supported by:

Acknowledgements

If someone offered me "GPCR purification…starting with DNA" as a PhD project today, I would run for the mountains (the mountains of Grenoble). Any success I have had with the project is at least in part due to the fantastic scientists I have had the good fortune to interact with. So that everyone is credited for the work they have done, acknowledgements are given at the beginning of each chapter in regards to the technical assistance I received to complete the work therein. That leaves me this whole section to acknowledge the people who have helped me, on a more personal level, to complete this PhD.

Professor Ted McMurchie, in particular, introduced me to science. The talk he gave me on the way home from a conference at Mawson Lakes in the final months of my Honours year was when I began to realise that science was a passion not a job – and I wanted in. Everything was possible with Ted and for the opportunities he allowed me I will be forever grateful.

Dr Ian Menz provided a much appreciated second opinion on everything related to my PhD. I always left meetings with Ian feeling enthused about my next experiment and confident in what I was doing. Ian was always encouraging and didn't offer the possibility that things wouldn't work out (including my estimation of how quickly I could get this thesis done).

If it wasn't for Dr Connie Darmanin I probably would have dwelled on whether my receptor purification was actually real for long enough to destroy the last year of my PhD. Furthermore, Connie was an excellent guide who, after recognizing my weakness for getting involved in too many experiments forcefully kept me focused on one project, the results even surprised me! It is a lesson I hope I have now learnt. No one through out my PhD has spent so much time teaching me, it has been an absolutely amazing experience learning from Connie and this thesis would have not come to be without her. I will be forever grateful to Connie for her help. As well as being a fantastic teacher, Connie is a wonderful friend. I also owe her thanks for the many nights of free accommodation at the beginning and the end of my time in Parkville, for finding me an apartment in Melbourne, for providing me with many "Nonna-like" meals and for the huge number of "giggles" that I shared with her.

Ted's second in command, Dr Wayne Leifert is a wonderful example of science for the love of it and it was always fun working with him. Wayne was an excellent source of advice on any experiment I could possibly imagine. His attitude of "what the hell, we might as well try" which applied to everything from emailing the big names to using an assay to see how potent his anti-histamine tablets were, is something that will stay with me throughout my career.

Dr Jose Varghese let me into his lab and made me one of two PhD students at the CSIRO Parkville site, for this I thank him. The third and fourth chapters of thesis would not have happened without the transfer to his project.

It seems like so long ago now but the original GPCR group in Adelaide really was special. Mrs Sharon Burnard, Ms Olgatina Bucco, Ms Kelly Bailey, Ms Tamara Cooper, Dr Janelle Williams and Dr Richard Glatz provided a wonderful, supportive work environment. Olgi always provided a friendly face and excellent conversation (both scientific and gossip ☺) in the first year and a half of my PhD. Olgi was also my graduating PhD role model and gave me confidence that maybe I was ok at science. Richard was always encouraging and the conversations we had over 'innoculatte' were fascinating. Also the CSIRO kintore avenue staff and students deserve acknowledgement for providing a supportive environment and excellently maintained facilities. In particular Peter Patterson (maintenance), Kaylene Pickering (OH&S), Leanne Griffiths (Librarian) and Milton Yates (IT), who worked "behind the scenes" to create an environment that ultimately meant I could spend more time in the lab.

Dr Ross Fernley and Dr Jenny Mckimm-Breshkin were kind enough to share their lab space with me in Parkville and Ross was particularly patient during my "transfer period" from a lab which consisted completely of messy, loud students to an organised, clean and quite lab. Ross's "yipees" when absorbance profiles started to peak are something I won't forget and I hope that I can maintain such enthusiasm throughout more career. Members of the Breshkin/Fernley laboratory became my Melbourne family and I am really grateful to know Mandy MacDonald, Sue Barratt, and of course Bec Attwood.

Abstract and summary of this thesis

This study describes expression, purification and crystallisation trials with three human seven transmembrane receptors (7TMRs).

A variety of Histidine (His) tagged constructs of the M_2 muscarinic receptor (M_2R) and a $5HT_{2A}$ serotonin receptor were prepared in baculovirus. A 10xHis tagged form of the human H_1 histamine receptor was obtained in recombinant baculovirus. M_2R, $5HT_{2A}R$ and H_1R constructs were expressed in $Sf9$ cells. Receptors expressed at between ~15 and 60pmol/mg of total membrane protein with the exception of the $5HT_{2A}R$ construct for which expression could not be conclusively demonstrated by radioligand binding. Two constructs were focused on; a C terminal 6xHis M_2R ($His6_CM_2R$) and the $His10_CH_1R$.

Membrane associated levels of the $His6_CM_2R$ and $His10_CH_1R$ were modulated by expression in the presence of receptor specific ligands. Addition of either atropine ($His6_CM_2R$) or triprolidine ($His10_CH_1R$) to receptor expressing $Sf9$ cells increased membrane associated receptor levels up to 3 fold.

G-protein subunits were purified by IMAC and used in $[^{35}S]$-GTPγS binding assays with the membrane bound $His6_CM_2R$ and $His10_CM_2R$. Addition of the 6xHis tag decreased the ability of the M_2R to activate $Gα_{i1}$ but did not render the receptor non-functional. Interestingly, $His10_CH_1R$ was also able to activate $Gα_{i1}$ with a 7 fold increase in $[^{35}S]$-GTPγS being observed in the presence of the agonist. This interaction between $His10_CH_1R$ has not been previously demonstrated in a cell-free system.

Solubilisation trials with $His6_CM_2R$ demonstrated n-Dodecyl-β-D-Maltoside (DDM) to be a useful detergent for extraction of the receptor from $Sf9$ membranes. A preliminary purification protocol for the receptor was developed using IMAC and GF-HPLC.

The $His10_CH_1R$ was solubilised using n-Octyl-β-D-glucopyranoside (nOG) with an estimated efficiency of 53% as determined by radioligand binding assay. Following IMAC, $His10_CH_1R$ was purified to homogeneity using GF-HPLC. The presence of antagonist throughout the purification was deemed as necessary for final recovery of the receptor but could not be conclusively removed from the receptor, making radioligand binding

measurements difficult. Addition of excess [3H]-ligand gave a functional recovery of the purified receptor of < 5% and a specific activity of ~500pmol/mg. Final yield of the receptor as determined by absorbance measurements was ~1mg from 5L of *Sf*9 cells (~ 2×10^6 cells/mL).

Two-dimensional crystal trials with the $His10_CH_1R$ were prepared by reconstitution of the receptor into the lipid mixture asolectin. Initially results for the 2D crystals appeared promising with ordered, lipidic areas generating electron diffraction patterns. However, an approximate calculation of the crystal unit cell of the 2D crystals demonstrated it to be too small to contain the receptor.

Three-dimensional trials with the $His10_CH_1R$ were carried out in the *meso* phase of either monoolein or phytantriol. Co-crystallisation trials with $His10_CH_1R$ and $G\alpha_{i1}$ produced clusters of needle-like crystals. These crystals were not formed in the presence of $G\alpha_{i1}$ only. A bunch of the crystals produced an X-ray diffraction pattern similar to that of a powder. Diffraction rings were visible at between 50Å and 3Å but it was not possible to index the diffraction pattern. Work with these crystals is on-going and they will be investigated at the Australian synchrotron later in the year.

Abbreviations commonly used in this thesis.

7TMR – Seven Transmembrane Receptor

AT_1R – Angiotensin 1 Receptor

CHAPS - 3-[(3-Cholamidopropyl)dimethylammonio]-1-propanesulfonate

CHO – Chinese Hamster Ovary

CSIRO – Commonwealth Scientific and Industrial Research Organisation

CSIRO MHT – CSIRO Molecular and Health Technologies

DDM – n-Dodecyl-β-D-Maltoside

DTAC – dodecyltrimethylammonium chloride

EC_{50} – half maximum effective concentration

$FPLC^{TM}$ Fast Protein Liquid Chromatography (from Pharmacia)

FRET – Fluorescence Resonance Energy Transfer

GDP – Guanosine DiPhosphate

GF-HPLC – Gel Filtration High Performance Liquid Chromatography

GPCR – G Protein Coupled Receptor

GTP – Guanosine TriPhosphate

H_1R – H_1 Histamine Receptor

HEK – Human Embryonic Kidney

$His10_CH_1R$ – C terminal, 10xHistidine tagged H_1 Histamine Receptor

$His6_CM_2R$ – C terminal, 6xHistidine tagged M_2 Muscarinic Receptor

IMAC – Immobilised Metal Affinity Chromatography

M_2R – M_2 Muscarinic Receptor

MQH_2O – milliQ treated water

NCMLS – Nijmegen Centre for Molecular Life Sciences, Nijmegen, The Netherlands

NMR – Nuclear Magnetic Resonance

nOG – *n*-Octyl-β-D-glucopyranoside

PCR – Polymerase Chain Reaction

PIP- phosphatidylinositol bisphosphate

POPC - 1-palmitoyl-2-oleoyl-*sn*-glycero-3-phosphocholine

QNB – 3-quinuclidinyl benzilate

RAMPs - Receptor Activity Modifying Proteins

SARDI – South Australian Research and Development Institute

SDS-PAGE – Sodium Dodecyl Sulfate PolyAcrylamide Gel Electrophoresis

Abbreviations commonly used in this thesis (cont...).

sMQH$_2$O – sterile miliQ treated water

SPR – Surface Plasmon Resonance

Throughout the thesis receptor-ligand binding is given in units of pmol/mg. This refers to pico-moles of ligand bound per mg of total cellular protein, unless otherwise stated in the text (for example pmol/mg of total membrane protein).

Table of Contents

Declaration

I certify that this thesis does not incorporate without acknowledgment any material previously submitted for a degree or diploma in any university; and that to the best of my knowledge and belief it does not contain any material previously published or written by another person except where due reference is made in the text.

Signed………………………………………….

Amanda Louise Aloia

Date……………………………………………..

1. Literature Review

1.1. Acknowledgements

I would like to thank Dr Connie Darmanin, Associate Professor Ted McMurchie and Dr Ian Menz for the carrying out the laborious task of reading and correcting my thesis. In particular I thank them for the way they all jumped to action to help me get this thesis finished within a strictly defined period of time. It was very much appreciated!

1.2. Introduction to Seven Transmembrane Receptors

Seven transmembrane receptors (7TMRs) are one of the primary mechanism by which extracellular signals are translated to the cytoplasm of the cell. Human 7TMRs are also known as G-Protein Coupled Receptors (GPCRs) due to their ubiquitous interaction with the intracellular G-proteins (Gα and βγ, Figure 1) (Hepler and Gilman, 1992; Leifert, et al., 2005a; Wess, 1997). There is evidence that 7TMRs can effect independently of the G-proteins (for a review, see (Kozasa, 2004)) and thus in this study the term 7TMRs will be used.
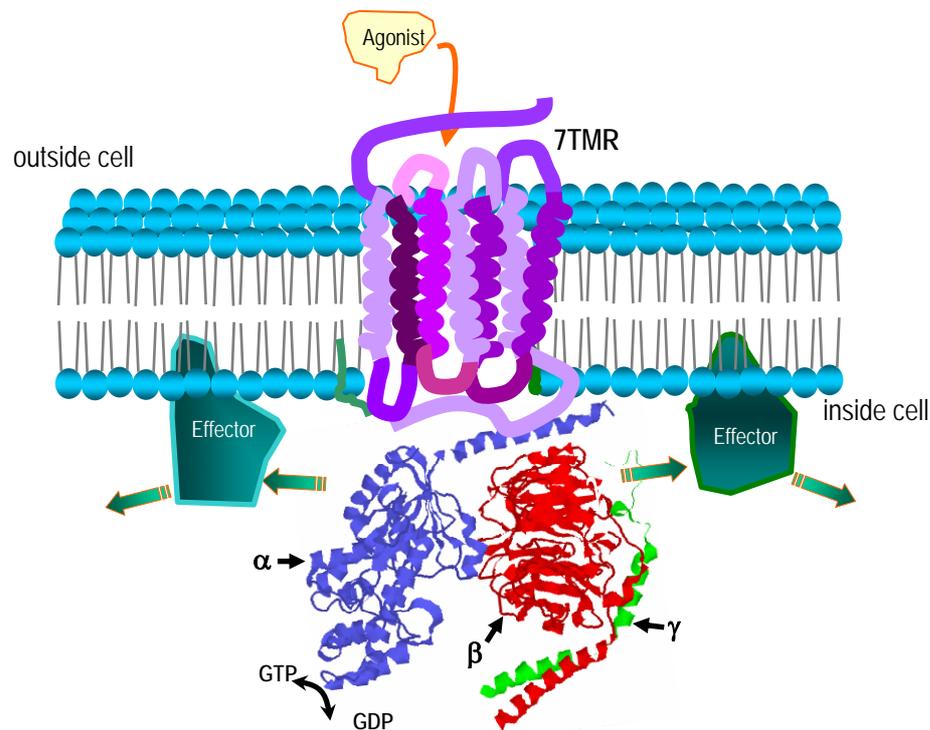
Figure 1. G Protein Coupled Receptor as a signal transducer. Agonist binding to the extracellular domain of the 7TMR stimulates GDP to GTP exchange on the intracellular Gα subunit; following which G proteins dissociate and activate down stream molecules; GTPase on the Gα subunit hydrolyses GTP back to GDP; G proteins reassociate and the system returns to basal state.

A simplified description of human 7TMR signal transduction is presented in Figure 1 in which an agonist binds to an extracellular site on the receptor promoting exchange of guanosine diphosphate (GDP) for guanosine triphosphate (GTP) on the intracellular Gα subunit and subsequent separation of the subunit from βγ (β and γ exist as a dimer) (De Lean, et al., 1980; Leifert, et al., 2005b; Neuwald, 2007). Both proteins go on to activate other molecules in the cell leading to a down stream physiological effect such as increase in blood pressure. The system returns to basal state when a GTPase on Gα hydrolyses GTP back to GDP and the G proteins reassociate.

Besides the G-proteins, there are a number of other proteins associated with the receptor that have an effect (directly or indirectly) on signalling. At the receptor level, arrestins and kinases play a regulatory role associated with receptor internalisation and desensitisation (Day, et al., 2004; Key, et al., 2005; Pfleger, et al., 2007; Reiter, et al., 2006). Receptor dimerisation and, in particular Receptor Activity Modifying Proteins (RAMPs), can have significant affect on receptor pharmacology (Milligan, et al., 2003; Morfis, et al., 2003; Park and Wells, 2003). At the G-protein level, Regulator of G-protein Signalling (RGS) proteins regulate the nucleotide binding proteins by accelerating the GTPase on $G\alpha$ (Chasse and Dohlman, 2003). The role of protein-protein interaction in 7TMR signalling has been reviewed very well elsewhere (Brady and Limbird, 2002; Milligan and White, 2001). The specificity (or lack there of) of receptor/G-protein interaction is another complex and intricate area of the 7TMR signalling pathway, a good review on this area has been written by Hermans, (2003).

1.2.1. Importance to Human Health

7TMRs are the most common cell signalling system in higher organisms and thus are particularly important in human health and disease (Marinissen and Gutkind, 2001). The involvement of 7TMRs in health and disease has attracted the research of pharmaceutical companies (see Table 1 for examples of prescription drugs which target 7TMRs) (Klabunde and Hessler, 2002). In 2005 approximately 60% of prescription drugs targeted 7TMRs (Lundstrom, 2005), a number that would be expected to increase with further research into receptor classes and subclasses. The human genome encodes for around 2000 7TMRs with approximately 210 of these having known natural ligands and only 30 being the target of current pharmaceuticals (Klabunde and Hessler, 2002). These statistics demonstrate the importance of research into 7TMRs in the search for new and/or improved therapeutics for a number of human diseases and conditions.

Table 1. Examples of prescription drugs that target 7TMRs, 30% of all prescribed drugs target 7TMRs.

Trademark Name	Generic Name	Condition	Receptor Targeted
Claritin	Loratadine	Allergies	H_1 (antagonist)
Atrovent	Ipratropium	Obstructive lung disease	M_2 (antagonist)
Risperdal	Risperidone	Schizophrenia	Dopamine (antagonist)
Duragesic	Fentanyl	Pain	Opioid (agonist)
Diovan	Valsartan	Hypertension	AT_1 (antagonist)

1.2.2. Seven Transmembrane Receptors - Structure and Function

7TMRs have an extracellular N terminus and seven transmembrane spanning segments linked by three intracellular and three extracellular loops (see Figure 2). The third intracellular loop is generally the largest (the length varies with receptor type), whilst the extracellular domains are relatively short (Milligan and White, 2001). Chimera studies have shown that receptor G-protein specificity is, at least in part, determined by the third intracellular loop of the 7TMR. It is this loop which is thought to be involved with receptor-kinase interaction. Good reviews on 7TMR structure have been written by Kobilka et al (2007) and Lagerström et al (2008).
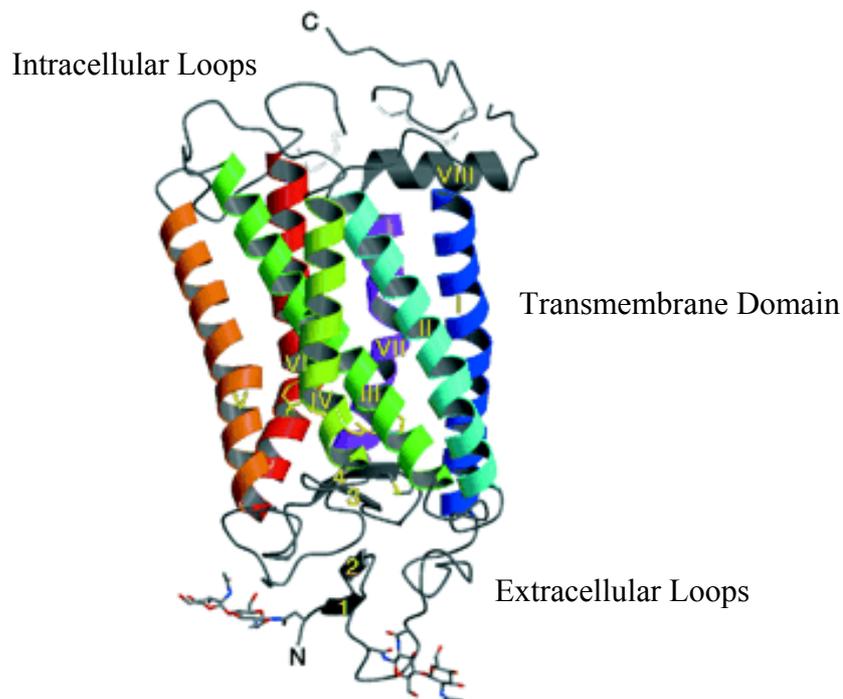
Figure 2. Ribbon structure of a representative 7TMR, Rhodopsin, showing seven transmembrane spanning segments, three intracellular and three extracellular loops. Image reproduced from (Palczewski, et al., 2000).

Until recently, a ligand to 7TMRs was described as being either an agonist, an antagonist or an inverse agonist depending on the effect caused to G-proteins. Agonist binding to a receptor leads to activation of the intracellular G-proteins and subsequent binding of GTP to Gα (as described in the 7TMR signalling section, Figure 1). Antagonist binding prevents the binding of agonist and essentially blocks activation of the G-proteins, leaving the 7TMR signalling system in a basal state. Inverse agonists are defined by their ability to block constitutive activity of receptor - activation of the G-proteins (or other signaling protein) that occurs in the absence of agonist binding. A change in terminology is beginning as mounting evidence suggests that all antagonists have some inverse agonist activity (Milligan and Bond, 1997).

There is evidence that 7TMRs may (or, in the case of the GABA$_b$ receptor, must) function as dimers or higher order oligomers. Such evidence has come primarily from co-immunoprecipitation studies, for example studies with the δ-opioid receptor. Cvejic and Devi (1997) co-expressed FLAG and c-Myc tagged forms of the receptor and used anti-cMyc immuno-chromatography followed by anti-FLAG Western blot to demonstrate that the receptor existed as homodimers. More recently, fluorescence resonance energy transfer (FRET) methods have been used to demonstrate the presence or receptor dimers (Latif, et al., 2001). FRET measurements have provided a more convincing argument for the functional relevance of 7TMR dimerisation as compared to co-immunoprecipitation techniques which may be more susceptible to artefacts (Salim, et al., 2002). For the α$_2$ and β$_1$ adrenergic receptors, dimersation has been shown to play a functional role in internalisation of the receptors (Xu, et al., 2003). Pfeiffer, et al., (2001) demonstrated that dimerisation of somatostatin 2A receptor with somatostatin 3 receptor lead to inactivation of the somatostatin 3 receptor. As more is learnt about the functional significance of 7TMR dimers the phenomonen may represent a novel target for pharmaceuticals, particularly if certain dimers form only in distinct tissue types. Dimers must be considered during 7TMR purification as they may alter perceived molecular weight, detergent solubilisation properties and chromatographic separations. Furthermore, the presence of 7TMR dimers may interfere with crystallisation.

Sequence analysis has been used to divide human 7TMRs into 5 families; the Glutamate, Rhodopsin, Adhesion, Secretin and Frizzled receptor families (Fredriksson, et al., 2003). The Rhodopsin family is the largest of the 5 groups and can be further subdivided into 13

clusters one of which is the amine receptor cluster.   In this study members of the amine receptor cluster, primarily the M_2 Muscarinic and the H_1 Histamine receptors, were investigated.

1.3.   The M_2 Muscarinic Receptor

The M_2 receptor (M_2R) belongs to a family of 5 Muscarinic receptor subtypes. The M_2 gene has been cloned from pig, rat and human, the later of which was used in this study.

1.3.1. Cellular/Physiological Functions

$[^{35}S]$-GTPγS assays using $M_2R$and purified G-protein subunits have shown coupling of the receptor to at least three different Gα subtypes including $Gα_o$, $Gα_z$ and $Gα_i$ (Parker, et al., 1991; Uustare, et al., 2004). Like the M_4 subtype, M_2Rs have the primary role of inhibiting the synthesis of cAMP, achieved through inhibition of adenylyl cyclase (Peralta, et al., 1988). Inhibition of adenylyl cyclase is caused by receptor activation of G-proteins of the $Gα_i$ class (the subscript i referring to inhibitory). The normal cAMP concentration in human cells is about $10^{-7}M$ but activation of muscarinic receptors can lead to a 20 fold decrease in this concentration in seconds (Alberts, et al., 1994). Similarly, activation of $Gα_z$ leads to inhibition of adenylyl cyclase (this G-protein is unique however in that it is pertussis toxin resistant, it also demonstrates a slower GDP-GTP exhange than $Gα_i$). Studies with M_2R and $Gα_z$ fusion proteins have demonstrated a role for the proteins in activation of K^+ channels (Vorobiov, et al., 2000). Studies with knock-out mice ($Gα_o$ -/-) have demonstrated the requirement for muscarinic receptor/$Gα_o$ interaction and the subsequent regulation of calcium channels in the heart (Valenzuela, et al., 1997).

M_2R is predominantly found in cardiac and smooth muscle. Ligand binding to the receptor in these tissues results in direct interaction of the activated G-proteins (in particular the βγ dimer) with K^+ channels (Mirshahi, et al., 2003). This leads to hyperpolarization of the heart and a subsequent drop in heart rate (as such, M_2 effects oppose those of the adrenergic receptors). The receptor is also found in the smooth muscle tissue of the bladder and has been implicated in disorders of the organ, such as overactive bladder syndrome (Mukerji, et al., 2006).

M_2 receptors have also been shown to activate the mitogen activated protein (MAP) kinase cascade (Crespo, et al., 1994).

1.3.2. Pharmacology

There are several known ligands for muscarinic 7TMRs. M_2 can be differentiated from other muscarinic receptors by relative affinities, for example the M_2 receptor has a low affinity for pirenzipine but a higher affinity for AF-DX 116[1], in comparison to the M_1 receptor (An, et al., 2002).

Agonists to the muscarinic receptor family are characterised by a quaternary Nitrogen (Figure 3). The nitrogen is believed to be important for interaction at an anionic aspartate residue located at the N terminal end of the third transmembrane domain (see section 1.3.3) (Huang, et al., 1999). The tertiary form of acetylcholine, dimethylaminoethylacetate, is 1000 fold less as effective as an agonist as the quaternary form, reflecting the potent effect of the quaternary nitrogen. Agonists to the M_2 receptor (and other muscarinic family members) include acetylcholine and carbachol, as well as the prototypical muscarinic agonist, muscarine.
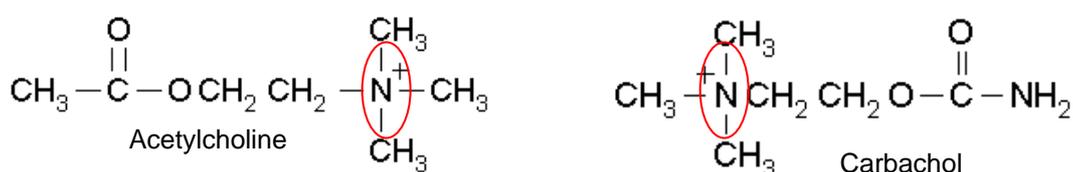
Figure 3. Structure of two commonly used Muscarinic receptor agonists, the quaternary nitrogen, a common feature of Muscarinic receptor agonists, is circled.

Scopolamine and atropine, two commonly used muscarinic antagonists are derived from a species of nightshade plant and are among the oldest known molecules originally derived from natural sources. Some studies have suggested that pirenzipine and atropine can behave as inverse agonists (Daeffler, et al., 1999; Jakubik, et al., 1995). For example, Jakubik, et al. (1995) used a cyclic [3H]-AMP assay to show an increase in cAMP production in (human) M_2 transfected CHO cells, with the addition of atropine (18% increase, EC_{50} 347 - 489pM).

---

[1] AF-DX 116 is an abbreviation of 11-([2-[(diethylamino)methyl]-1-piperdinyl]acetyl)-5, 11- dihydro-6H-pyrido[2,3-b][1,4]benzodiaze pine-6-one.

A table of commercially available muscarinic receptor ligands is shown in Table 2.

Table 2. Table of commercially available M_2 Muscarinic and general Muscarinic ligands. Adapted from Sigma Aldrich website. Names of example structures shown are designated by *___*.

Ligand Type	Examples	Example Structure
M_2R selective agonist	*Bethanechol* (selective relative to M_4R)	
M_2R selective antagonists	Methoctramine AF-DX 116 AF-DX 384 Gallamine *Himbacine* Triptramine	
General muscarinic receptor agonists	Acetylcholine Carbachol Bethanechol *Muscarine* Metoclopramide Pilocarpine Oxotremorine	
General muscarinic receptor antagonists	Scopolamine QNB *Atropine*	
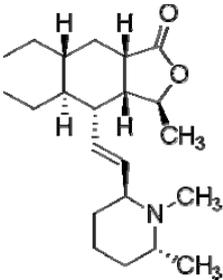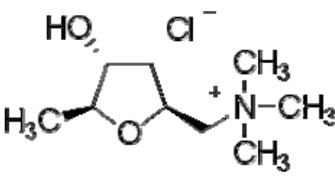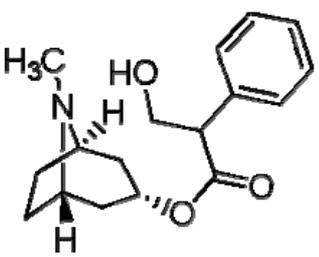
1.3.3. Structure/Function

The human M_2R is represented by 1398 DNA base pairs, encoding for a 466 amino acid protein (Figure 4). Points of interest on the amino acid sequence, as well as putative positions of the loops and transmembrane segments, are shown in Figure 4. Like other members of the Rhodopsin family of 7TMRs, the muscarinic family is characterised by a

large third intracellular domain (amino acids 208 – 388, Figure 4). It is within this region that G-protein specificity is defined and the two classes of muscarinic receptor (i.e M_2/M_4 and $M_{1,3 \text{ and } 5}$) are characterised. The M_2 muscarinic receptor can be defined from other receptor types by a seven element fingerprint (i.e. 7 different amino acid sequences). The first element of the fingerprint lies at the N terminal region of the receptor (amino acids 7-23), the remaining 6 elements reside in the third intracellular loop, again confirming the importance of this region in receptor function. Comparatively however, the muscarinic receptor family is highly conserved in amino acid sequence (more so than the α adrenergic receptor family) and this has led to difficulty in developing ligands which are selective between the individual subtypes in the family.

```
1                    22                      45          59
MNNSTNSSNNSLALTSPYKTFEVVFIVLVAGSLSLVTIIGNILVMVSIKVNRHLQTVNNYFLFSLACADLIIG
       80              97               119              139
VFSMNLYTLYTVIGYWPLGPVVCDLWLALDYVVSNASVMNLLIISFDRYFCVTKPLTYPVKRTTKMAGMMIAA
         162               184                   207          219
AWVLSFILWAPAILFWQFIVGVRTVEDGECYIQFFSNAAVTFGTAIAAFYLPVIIMTVLYWHISRASKSRIKK
                                                                 292
DKKEPVANQDPVSPSLVQGRIVKPNNNNMPSSDDGLEHNKIQNGKAPRDPVTENCVQGEEKESSNDSTSVSAV
         307
ASNMRDDEITQDENTVSTSLGHSKDENSKQTCIRIGTKTPKSDSCTPTNTTVEVVGSSGQNGDEKQNIVARKI
            388                  409           423
VKMTKQPAKKKPPPSREKKVTRTILAILLAFIITWAPYNVMVLINTFCAPCIPNTVWTIGYWLCYINSTINPA
   443                  466
CYALCNATFKKTFKHLLMCHYKNIGATR
```

Figure 4. Amino acid sequence of the human M_2 Muscarinic Receptor showing regions of interest. Red letters represent extracellular loops, blue letters transmembrane domains and light green letters the cytoplasmic loops. Potential sites of glycosylation are highlighted in bold green (van Koppen and Nathanson, 1990). Potential phosphorylation sites are highlighted yellow (Lee, et al., 2000). The sequence highlighted in grey is involved in $G\alpha_i$ coupling, replacement with the equivalent sequence from M_3 removes pertussis toxin sensitive signalling (Bonner, 1992).

Mammalian 7TMRs are glycosylated, the muscarinic receptor in particular is heavily glycosylated, with up to 50% of receptor mass being comprised of carbohydrate in cardiac muscarinic receptors. Based on sequence, the human M_2R has 4 potential glycosylation sites (Asn – X – Ser/Thr) at amino acids 2, 3, 6 and 9. Mutagenesis studies at Asn^2, Asn^3 and Asn^6 on M_2 receptors expressed in CHO cells have shown that glycosylation is not required for localisation of receptor to the cell membrane or antagonist ([3H]-NMS and [3H]-QNB) binding (van Koppen and Nathanson, 1990).

Phosphorylation of 7TMRs occurs through the activation of the second messenger dependent kinases (PKA or PKC) or through 7TMR kinases (GRK). Phosphorylation by

GRK is dependent on agonist activation. In the cell, phosphorylation is required to recruit the adapter proteins, arrestins. In turn, arrestins are involved in receptor desensitisation by aiding in the prevention of G-protein interaction and coupling to clathrin coated pits for endocytosis. Three amino acids are able to be phosphorylated; Serine (Ser), Threonine (Thr) and Tyrosine (Tyr). Phosphorylation at Tyr is quite rare and, to date, does not appear to be implicated in M_2 Muscarinic Receptor phosphorylation. In the M_2R there are two phosphorytable "clusters" containing a number of Ser and Thr amino acids (Figure 4, highlighted in yellow). Unlike other members of the rhodopsin-like family of 7TMRs such as rhodopsin and β_1 adrenergic, which are phosphorylated at the C terminus, the phosphorylatable clusters of the M_2R are located in the third intracellular loop at amino acids 286-290 and 307-311 (Pals-Rylaarsdam and Hosey, 1997). Mutation of Ser and Thr in both of these clusters prevents phosphorylation of the receptor which occurs in response to prolonged agonist exposure, this phosphorylation event usually decreases the ability of the receptor to activate its signalling pathways. However, the two phosphorylation clusters are thought to act in an independent manner (Pals-Rylaarsdam and Hosey, 1997). Mutagenesis studies of the acidic amino acids (Asp and Glu) either side of the Ser/Thr cluster have suggested them to be a part of the consensus sequence for required for GRKs, as well as being important in 7TMR/arrestin interactions (Lee, et al., 2000). Interestingly, mutations performed at these sites (amino acids 286-290, 298-300, 304-305 and 307-311) did not effect receptor/G-protein coupling (as shown by an intact ability to activate potassium channels), despite the fact that the sequences reside in the third intracellular loop.

Mutagenesis studies have shown that the C terminal Cys^{457} is a site of palmitoylation in the M_2R. Receptors which were mutated at this point retained the ability to interact with GRK2, however, when reconstituted with G-proteins ($G\alpha_{i2}$), the extent of $[^{35}S]$-GTPγS binding was 50% less than in the wild type (Hayashi and Haga, 1997).

The ligand interaction sites for M_2 receptors can be drawn from homology with the other muscarinic receptors. Molecular modelling studies suggest that Asp^{103} in the third transmembrane domain, Thr^{190} in the fifth transmembrane domain and Asn^{404} in the sixth transmembrane domain, sites which are conserved throughout the muscarinic family (amino acid positions given are for the human M_2R), are involved in agonist binding (Huang, et al., 1999). In particular the Asp residue is highly conserved amongst receptors

that bind biogenic amines with this negatively charged amino acid allowing for interaction with positively charged quarternary amines found in muscarinic agonists. In addition mutagensis studies on the M_1 receptor have shown that Thr^{192} (transmembrane five) and Asn^{382} (third intracellular loop) play an important role in agonist binding with both of these sites being conserved amongst the muscarinic family (Huang, et al., 1999). Asn^{382} is also involved in antagonist binding to the receptor (Huang, et al., 1999).

Several good reviews of muscarinic receptor structure have been written (Hulme, et al., 1990; Hulme, et al., 2003; Goodwin, et al., 2007).

1.4.   The H_1 Histamine Receptor

1.4.1. Cellular/Physiological Functions

H_1 histamine receptors (H_1Rs) are widely distributed in the human body and have been located in the gastrointestinal tissue (Sander, et al., 2006), cartilage (Tetlow and Woolley, 2005), the brain (Kitanaka, et al., 2007), the nasal mucosa (Murata, et al., 2004) as well as the placenta (Matsuyama, et al., 2006).

Differences in H_1R binding potentials between healthy and neuropsyhciatric disorder patients has demonstrated a role for the H_1R in Alzheimers, schizophrenia and depression (Tashiro and Yanai, 2007). Through blockade of the H_1R, anti-histamines are used in the treatment of allergies (Simons, 2004) and motion sickness (Shupak and Gordon, 2006).

Several studies have demonstrated an interaction of the H_1 histamine receptor (H_1R) with members of the $G\alpha_q$ family, by measurement of inositol phosphate production in stably expressing CHO cells (Leurs, et al., 1994b), direction of antibodies to a $G\alpha_q$ subunit (Gutowski, et al., 1991) and Ca^{2+} ion measurement (Leopoldt, et al., 1997). Activation of $G\alpha_q$ results in the activation of phospholipase C which then converts phosphatidylinositol bisphosphate (PIP_2) to diacylglycerol (DAG) and inositol triphosphate (IP_3). DAG activates protein kinase C (PKC) which may be involved in desensitisation of H_1R (Smit, et al., 1992). IP_3 formation leads to the release of calcium from intracellular stores and an influx of calcium from the extracellular environment. There is some evidence that H_1R may also couple to pertussis-toxin sensitive $G\alpha_i$ (Seifert, et al., 1994).

1.4.2. Pharmacology

In the body, L-Histidine is converted to histamine by the enzyme Histidine decarboxylase (Figure 5). The naturally produced histamine receptor agonist is involved in numerous physiological processes as described above. In particular through the H_1R, the functions of histamine include the sleep-wake cycle, cognition, memory, inflammation and allergies (Simons, 2004). It follows that there are greater than 40 inverse agonists (anti-histamines) for the H_1R that are in clinical use (Simons, 2004).
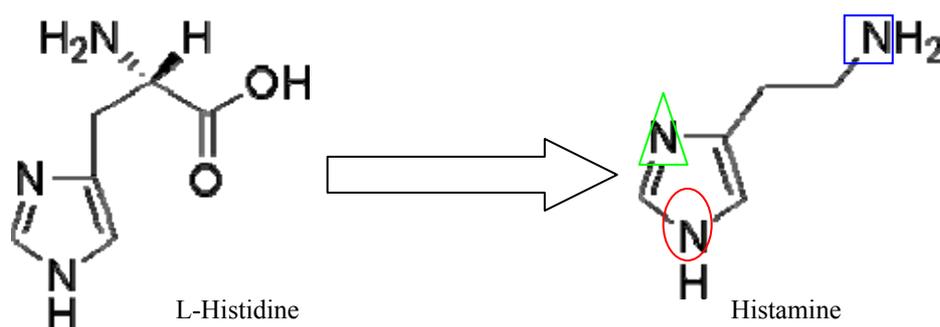
Figure 5. L-Histidine is converted to histamine by the enzyme Histidine decarboxylase. The circled nitrogen is involved in binding to Asp[207] of transmembrane five, the boxed N with Asp[107] and the triangle enclosed N with Lys[200], as described in the text.

Anti-histamines are primarily from six chemical groups as shown in Table 3. Early anti-histamines (clinically classified as 'first generation' drugs) have the side-effect of causing drowsiness. These drugs were predominantly discovered by random screening, examples include pyrilamine (used for the treatment of insomnia) and hydroxyzine (allergy and nausea). The drowsiness effect of first generation anti-histamines is a result of the small, lipophilic drugs being able to cross the blood brain barrier (BBB). This phenomenon was demonstrated neatly by (Okamura, et al., 2000) who used competition between chlorpheniramine and [11C]-doxepin, in combination with positron emission topography to determine the percentage of H_1R occupied in the brain when subjects were treated with a therapeutic dose of the unlabelled drug. So called second generation anti-histamines, such as loratadine (allergies) and cetirizine (allergies) are the result of slight chemical modifications to the first generation drugs, for example cetrizine is metabolite of hydroxyzine. Second generation anti-histamines are predominantly targeted to non-central nervous system H_1Rs and thus do not tend to cause severe drowsiness.

Isomerism plays an important role in the potency of a number of H_1R inverse agonists, in particular for those based on alkylamine chemistry. The trans- isomer of triprolidine is 1000 times more active than the cis- isomer. As with all 7TMR targeting drugs, the problem of unwanted side-effects remains due to the lack of specific receptor binding. Anti-histamines are no exception. In particular, first generation anti-histamines can interfere with muscarinic, adrenergic and serotonin receptors, resulting in side effects such as dry mouth, hypotension and increased appetite (Simons, 2004).

Table 3. H$_1$ histamine receptor inverse agonists. The inverse agonists can be grouped according to their structural basis. All ligands shown here are (or have previously been) used in the treatment of allergies. Only first generation anti-histamines are capable of passing the BBB.

Chemical Basis	Examples	Structure Example
Alkylamine group R-NH$_n$	brompheniramine chlorpheniramine dexchlorpheniramine	Triprolidine (hydrochloride)
Ethanolamine group HO—CH$_2$CH$_2$—NH$_2$ Able to cross BBB	doxylamine carbinoxamine clemastine	Clemastine
Ethylenediamine group H$_2$N—CH$_2$CH$_2$—NH$_2$ Able to cross BBB	antazoline tripelennamine pyrilamine	Pyrilamine
Phenothiazine group Able to cross BBB	methdilazine promethazine	Promethazine (hydrochloride)
Piperazine group Some able to cross BBB	cyclizine hydrozine oxatomide	Cetirizine (dihydrochloride)
Piperidine group	desloratadine fexofenadine mizolastine olopatadine	Loratadine
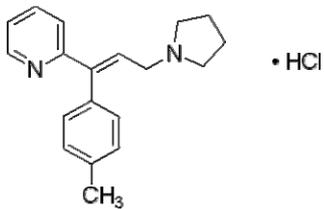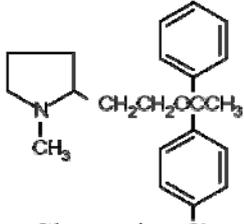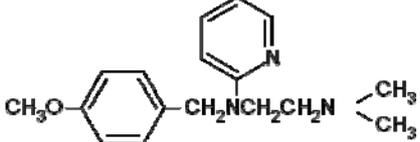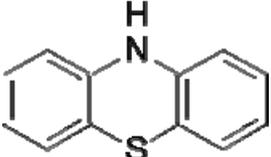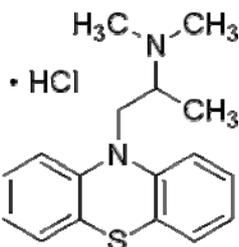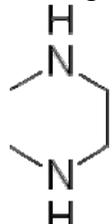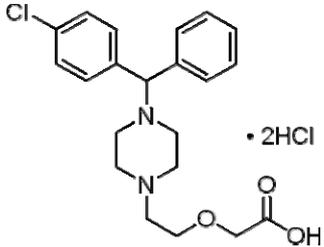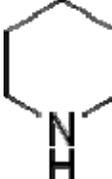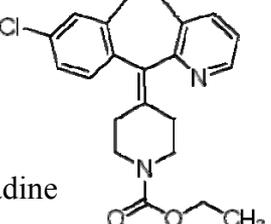
1.4.3. Structure and Function

The human H_1R consists of 487 amino acids encoded for by a 1461 base pair coding sequence, the gene of which is located on chromosome 3 (Moguilevsky, et al., 1994). From the amino acid sequence, the receptor has a calculated molecular weight of approximately 56kDa. The family has low amino acid sequence homology between its members, often showing greater similarity to other amine receptors (Zhu, et al., 2001). The human H_1 receptor shares 22% with human H_3R but around 45% homology with some members of the muscarinic receptor family (Simons, 2004).

Analysis of the amino acid sequence shows two possible glycosylation sites at Asn^5 and Asn^{18}. SDS-PAGE analysis of $[^3H]$-pyrilamine binding sites in cultured smooth muscle cells showed a protein of 68-97kDa (Mitsuhashi and Payan, 1989). Treatment with glycanase reduced the size of the $[^3H]$-pyrilamine binding site to 40kDa, a lower than expected value which the authors attributed to proteolytic cleavage. Kuno, et al., (1985) used a unique method of 'target size analysis', or radiation inactivation, to suggest the presence of a 160kDa $[^3H]$-pyrilamine binding site in both the bovine and human brain. The $[^3H]$-pyrilamine binding site may represent glycosylated (or dimerised) histamine receptor. Most convincing however, is a recent report by Sansuk, et al., (2008) who used MALDI-ToF MS to analyse a tryptic digest of human H_1 histamine receptor before and after treatment with the glycosylase PNGase, which cleaves N-linked glycosylation at asparagine. The analysis demonstrated that human H_1 histamine receptor, produced using the baculovirus/*Sf9* cell expression system, was glyosylated at Asn^5 but not at Asn^{18}

Potential phosphorylation sites are located at Thr^{60}, Ser^{396} and Thr^{478} (Moguilevsky, et al., 1994). H_1R signalling through $G\alpha_q$ results in the activation of PKC (as previously described). Phosphorylation of the receptor by PKC begins receptor densitization or down-regulation and is a required initial step of receptor desensitization with receptors lacking phosphorylation sites failing to be downregulated by excess agonist activation (Miyoshi, et al., 2006). Miyoshi, et al., (2004) demonstrated a relationship between M_3 muscarinic receptor activation and H_1R phosphorylation by PKC, a neat example of the interaction between 7TMRs of different classifications.

Like other amine binding 7TMRs, the Aspartate residue in transmembrane III (Asp^{106} in

H_1R) is involved in the binding of ligand amino groups (Ohta, et al., 1994). Furthermore, mutagenesis studies have shown a requirement of Asn^{198} (transmembrane V) in agonist binding (Ohta, et al., 1994). Investigations by Leurs, et al., (1994a) have neatly demonstrated the specific roles of particular amino acids in the H_1R by mutation of residues in question, as well as measurement of IP production following treatment with various receptor ligands. Thr^{203} was shown not to be involved in histamine binding, whilst Asp^{207} of transmembrane V is involved in histamine interaction through the Nitrogen as shown in Figure 5. Further studies demonstrated a role of Lys^{200} for the binding of histamine but not pyrilamine (Leurs, et al., 1995). Interestingly, Lys^{200} was shown to interact with a different Nitrogen of Histamine than Asp^{207} (Figure 5) (Leurs, et al., 1995). Mutational studies have also been combined with computational models of H_1R ligand binding in order to determine the role of particular amino acids (Jongejan, et al., 2005). Models for the histamine receptor were based on the crystal structure of rhodopsin however, and so this method may benefit further from the recent structures of the β_2-adrenergic receptor (Cherezov, et al., 2007; Rasmussen, et al., 2007). Whilst mutational studies may be considered to provide circumstantial evidence to the role of particular amino acids, NMR studies have also shown the involvement of Asp^{106} in binding of histamine to a purified H_1R (Ratnala, et al., 2007).

1.5.   7TMR Assays

There are a number of assay systems related to the study of 7TMRs. Broadly these can be divided into those which analyse receptor-ligand binding only and those which analyse activation of the G-proteins. In both cases cellular and cell-free systems are possible. The variety of detection techniques used to assay 7TMRs (for example surface plasmon resonance, fluorescence polarisation and fluorescence resonance energy transfer) in and out of the cell are too numerous to review here, but have been previously reviewed in great detail (Leifert, et al., 2005a). There are two assays of importance for the focus of the study presented here; ligand binding and G-protein signalling assays.

Ligand Binding - the design of this assay system resulted in breakthroughs in pharmacological studies of 7TMRs (Lefkowitz, 2004). Using a labelled ligand (generally radioactive, though more recently fluorescent molecules have been used) a large amount of useful information can be gained about the receptor of interest. For this study, saturation binding assays allow determination of receptor expression (mol/mg). Verification of

receptor subtype can be achieved by K_d determination and competition curves (unlabelled ligand of increasing concentration is competed against a fixed concentration of labelled ligand, see Figure 6) giving EC_{50} values for various ligands. Assaying for ligand binding is also an initial step in confirming receptor functionality, particularly during and after solubilisation and purification protocols.

Signalling Assays are defined here as those which detect G-protein activation. This may be achieved in a number of ways (Leifert, et al., 2005a), of importance here is (cell free) [^{35}S]-GTPγS binding to Gα. In terms of receptor functionality, signalling assays allow for full assessment by showing that the receptor is capable of both binding agonist and activating G-proteins. In relation to drug discovery, signalling assays offer an advantage in that ligands can be distinguished as agonist, antagonist or inverse agonist. The [^{35}S]-GTPγS binding assay has had extensive use in the 7TMR field (DeLapp, 2004; Harrison and Traynor, 2003; Jasper, et al., 1998; Milligan, 2003). The assay employs a non hydrolysable, radioactive GTP such that the binding of the [^{35}S]-GTPγS to Gα (on activation by agonist bound receptor) is non reversible and can consequently be detected by scintillation counting.
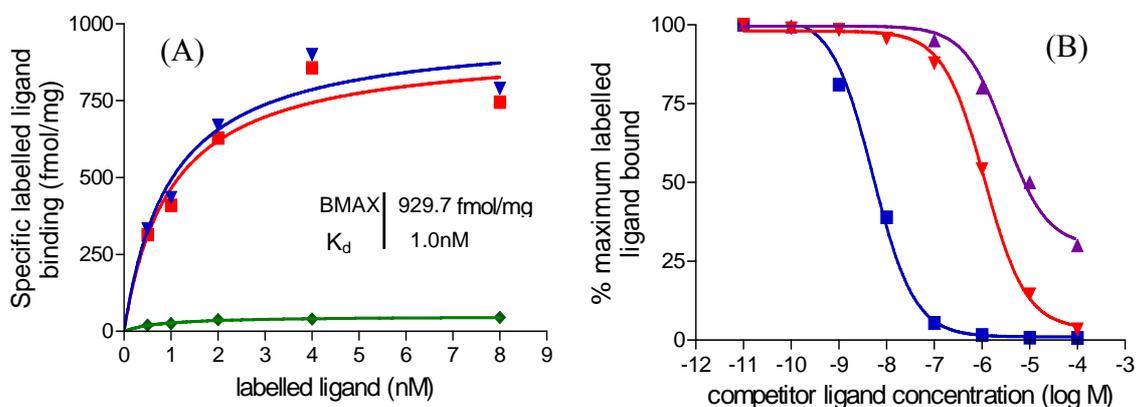
Figure 6. Representative Saturation and Competition Binding Assays. (A) In a saturation assay an increasing concentration of labelled ligand is added to the receptor preparation (blue triangle). Addition of an excess concentration of competing un-labelled ligand (green diamond) gives non-specific binding of the labelled ligand. Specific binding (red square) is then calculated by subtracting non-specific from total. B_{max} gives a measure of receptor concentration, K_d of receptor affinity for ligand. (B) Competition binding uses a fixed concentration of labelled ligand against log increases of un-labelled ligand. The EC_{50} value represents the un-labelled ligand concentration at which half maximal labelled ligand is bound. For ligand 1 (blue squares) the EC_{50} is 5.2nM, for ligand 2 (red triangles) the EC_{50} is 1.1µM and for ligand 3 (purple triangles) the EC_{50} is 3.1µM.

1.6. 7TMR Expression

Techniques allowing for over-expression of a protein of interest have greatly enhanced the ability to study and purify G protein coupled receptors. For the production of protein, over expressing cell culture is a great improvement since the days when huge quantities of tissue were required to yield a comparatively small amount of final protein product (Caron, et al., 1979; Cerione, et al., 1983; Shorr, et al., 1982). Overexpression of 7TMRs has been achieved in yeast, *E. coli*, mammalian cells and insect cells. Of the yeast organisms, *Saccharomyces cerevisae* and *Schizosaccharomyces pombe* have been used, producing expression levels in excess of 10pmol/mg (Reilander and Weiss, 1998). An advantage of using yeast is its adaptability to large scale culture. Furthermore, post-translational modifications are performed similarly to mammalian cells, though N-glycosylation appears to be inefficient (Tate and Grisshammer, 1996). *E. coli* is also easily adapted to rapid growth, large scale culture. The major drawback for *E. coli* expression however, is the inability of the prokaryotic bacterium to perform post-translational modifications, such as glycosylation and phosphorylation. Furthermore, some research has shown that native *E. coli* strains cannot simultaneously produce new membrane environments whilst synthesising receptor protein (Arechaga, et al., 2000). Despite this some 7TMRs have been expressed in *E.coli*. In one such study a C terminal Histidine tagged M_2 muscarinic receptor was expressed in *E. coli* (Furukawa and Haga, 2000). The receptor was fused to maltose binding protein at the N terminus and contained a deletion in the third intracellular loop, however, [^{3}H]-QNB binding was comparable between receptors expressed in *E. coli* and those expressed in *Sf9* insect cells. The authors also suggest that the purified receptor was capable of interaction with G-proteins (as shown by carbachol stimulated [^{35}S]-GTPγS binding). A different bacterium which presents interesting properties for 7TMR expression is the photosynthetic bacteria *Rhodobacter*. *Rhodobacter* express proteins involved in photosynthesis in internal membrane structures which are produced in large amounts under inducible growth conditions. Laible, et al., (2004) have utilised these properties to harvest integral membrane proteins. The plasmid transfected bacterium are grown under semi-aerobic conditions, the lack of oxygen inducing co-ordinated protein expression and membrane synthesis. Intracellular membrane structures are separated from lysed cells by differential centrifugation. The authors then went on to detergent extract the His-tagged protein and subsequently purify it by use of FPLC^{TM} and gel filtration or ion exchange chromatography. Though this technique appears to be in the early stages of development, it

may prove a useful technique for 7TMR production, particularly if expression of native proteins in the intracytoplasmic membranes can be halted and replaced with a desired recombinant protein thus negating the need for long and difficult purification protocols. However, the limitations of prokaryotic post-translational modification would still exist. Yoshino, et al., (2004) utilised intracellular bacterial magnetic particles produced by the interesting bacterium *Manetospirillum magneticum*. The bacteria produce nanosized particles of Fe_3O_4 coated with a protein/lipid bilayer, these "magnetosomes" can thus be separated from the bacterium using a magnetic column. Proteins reside in the membrane of the magnetosome and the authors utilised a protein known as Mms16 (the most abundantly expressed protein in the membrane) as an anchor/attachment point for the D_1 Dopamine receptor. The plasmid was constructed with the C terminus of the Mms 16 sequence aligned with C terminus of the D_1 gene. The plasmid was transfected into the magnetic bacteria and the magnetosomes subsequently purified out. Specific binding of a D_1 ligand was shown, though there was a high degree of non-specific binding in magnetosomes from untransformed bacteria and receptor expression levels appeared to be low. Though an interesting technique the process would have limitations in that the use of a prokaryote for expression would limit posttranslational modifications of the receptor and reconstitution of the 7TMR with G-proteins may be difficult. Finally, although the receptor is not in a purified membrane environment it is likely an improvement on receptors expressed in typical cell cultures as Mms16 seems to be the dominant protein in the intracellular membranes. This, along with the inherent magnetic properties of the particles, may prove this to be a useful technique subject to further research and modifications.

Mammalian cell lines provide an environment most similar to the native receptor environment in the tissue of higher organisms. There are a number of stably transfected mammalian cell lines available for 7TMR expression including CHO, HEK and Cos (Jakubik, et al., 1995; Ramsay, et al., 2002). The major disadvantage of mammalian cell lines is the large time requirements for maintenance and difficulty in achieving large (mg) quantities of functionally expressed protein in large scale cultures (e.g. in bioreactors). Furthermore, scaling up of mammalian cultures is laborious and costly (Stanasila, et al., 1998). However, several 7TMRs have been expressed in mammalian cell lines, including the M_2R (Peterson, et al., 1995) and the H_1R (Miyoshi, et al., 2006) both of which have been expressed in CHO cells at reasonable levels, though the reported expression of M_2R was particularly high at 50pmol/mg and this work does not appear to have been replicated.

In general, expression of GPCRs in mammalian cells does not reach levels of more than 5-10 pmol/mg total cellular protein (Massotte, 2003). An exception to this expression level limit has been demonstrated for the β_2 adrenergic receptor in tetracycline inducible HEK293 cells (Chelikani, et al., 2006). A Kozak sequence and bovine rhodopsin tag were added and codon optimisation (increase in GC content) was performed on the receptor sequence. Expression level of the receptor reached 220pmol/mg as determined by [^{3}H]-dihydroalprenolol binding to the HEK cell membranes. Further, the unmodified receptor could be expressed in COS-1 cells to levels of 18pmol/mg total cellular protein (Chelikani, et al., 2006). Reeves et al (2007), produced a tetracycline inducible HEK293 cell line which lacked N-acetylglucosaminyl-transferase-I and so was unable to perform complex N-glycosylation. Expression of rhodopsin in this cell line reached levels of 6mg per litre of cell culture and, perhaps more importantly for crystallisation studies, the receptor was homogenous with respect to glycosylation. Infection with recombinant Semliki Forest virus has also been used to express 101 different 7TMRs in mammalian cells (Hassaine, et al., 2006). The human adenosine receptor demonstrated the highest expression level of the receptors tested at 287pmol per mg of total cellular protein. A potential limitation of this method of expression is the cost which is high compared to other mammalian systems.

An alternative to the expression systems previously described is the baculovirus/insect cell expression system, which is easily and comparatively inexpensively scaled up to large scale cultures. In this expression system, a cDNA encoding the protein is ligated into a transfer plasmid that is subsequently relocated into the baculovirus (in this case *Autographa californica* multiple polyhedrosis virus). In this study, the Bac-to-Bac$^®$ baculovirus construction system from Invitrogen was used (see Figure 7). Replacement of the polyhedrin gene in baculovirus DNA with the gene of interest allows for high levels of expression of the target gene. The polyhedrin promoter is a late promoter, beginning at approximately 24 hours post infection (pi), peaking at 48-72 hours pi and with significant cell death occurring at 4-5 days pi.
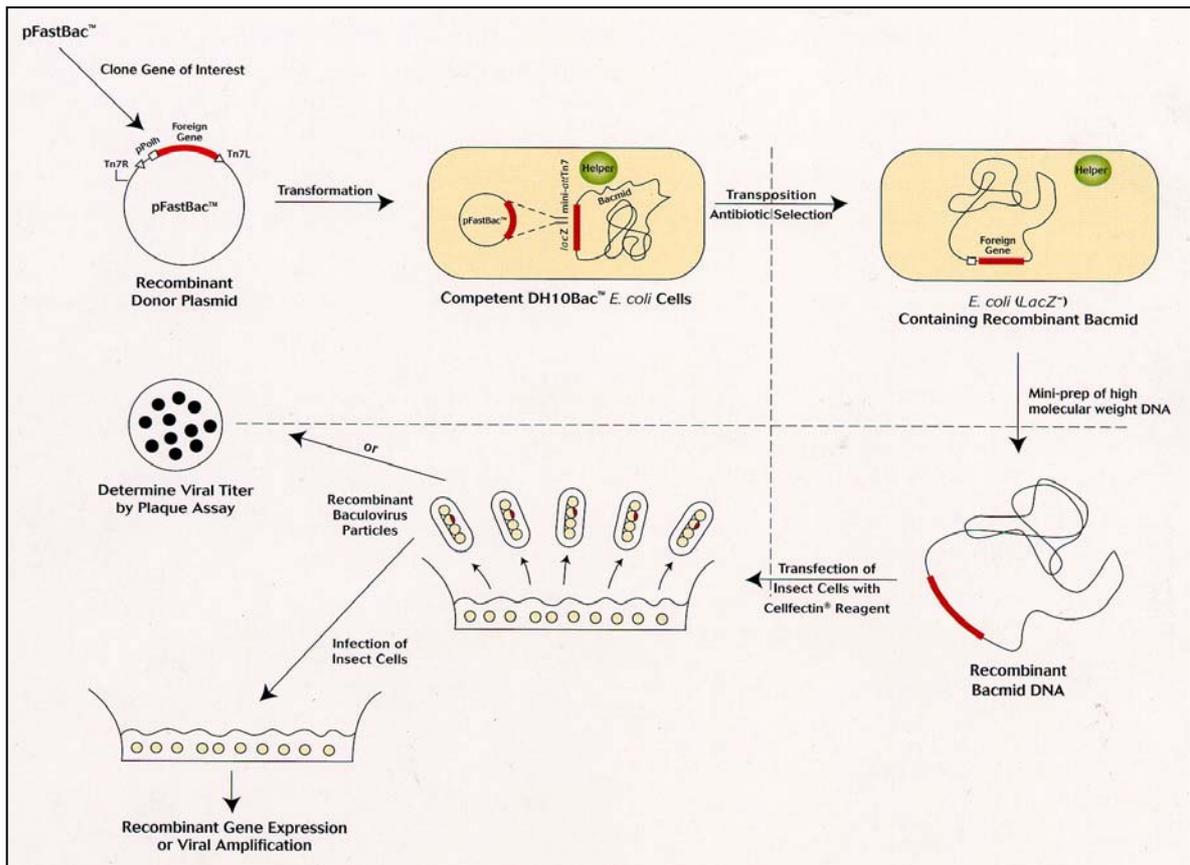
Figure 7. Construction of a recombinant baculovirus using the Bac-to-Bac® baculovirus expression system from Invitrogen. Gene of interest is digested with recombinant donor plasmid. This plasmid is incubated with DH10Bac *E. coli* cells, a specially constructed cell line containing baculovirus DNA, a "helper" plasmid (proprietary technology) aids transfer of gene of interest into baculovirus DNA, within the *E. coli* cell. High molecular weight (i.e baculovirus) DNA is collected from selected *E. coli* cells. Transfection of insect cells with the baculovirus DNA produces recombinant baculovirus containing gene of interest.

There are two insect cell lines commonly used; *Spodoptera frugiperda 9* (*Sf9*) or *Sf21* both are derived from the ovarian cells of the insect. Though insect cells can achieve most post-translational modifications, only simple glycosylation appears to take place (Jarvis and Finn, 1995). A number of 7TMRs have been successfully expressed (production in the range of pmol/mg total cellular protein) in *Sf* insect cells, including M_2 muscarinic, bovine rhodopsin, β-adrenergic and the H_1 histamine receptor (Hayashi and Haga, 1996; Janssen, et al., 1995; Kobilka, 1995; Ratnala et al., 2004).

Though current cell expression techniques have drastically improved the amount and speed at which functional integral membrane proteins can be produced, the technique inherently means that for most structural and functional assay studies, the protein will need to be solubilised and purified from the plethora of native proteins which inhabit the membrane.

The intrinsic difficulties in removing the 7TMR from its native membrane environment during classical purification protocols could be negated by the use of a protein synthesis system which only produces the protein of interest. Cell free synthesis utilises components taken from either a prokaryotic source (e.g. *E. coli*), eukaryotic source such as rabbit reticulate lysate or wheat germ extract, to translate protein from mRNA (or in some cases DNA). The crude extract containing all the necessary translational requirements is combined with a supply of amino acids, nucleotides (if starting material is DNA) and molecules required for energy generation (ATP, GTP etc.). The first cell free protein synthesis producing protein in high yields was reported in 1988 (Spirin, et al., 1988). Spirin, et al., (1988) significantly advanced the field with the development of continuous cell-free translation, in which reaction products are continuously removed from the reaction mixture and consumable reactants (ATP, amino acids) are restored. This method allowed the researchers to report constant synthesis times of tens of hours resulting in hundreds of synthesised peptides using both *E. coli* and wheat germ based cell extracts. Technical details of cell free synthesis will not be reviewed in detail here but there are several good papers discussing this topic (Endo and Sawasaki, 2004; Jackson, et al., 2004; Spirin, 2004). Several 7TMRs have been expressed in a cell free system (Klammt, et al., 2007). Early work by Kobilka, (1990) used a rabbit reticulocyte lysate, to translate β_2 Adrenergic receptor mRNA, combined with membrane preparations prepared from *Xenopus laevis* oocytes (which contain few β_2 receptors). The 52kDa protein produced was somewhat smaller than the 80kDa β_2 adrenergic receptor that is produced in mammalian cells, suggesting incomplete glycosylation. Though the report suggested that, when synthesised in the presence of the membrane preparation, the *in vitro* system was capable of producing some glycosylation. Impressively, the protein product of *in vitro* translation of the β_2 adrenergic gene showed saturable ^{125}I-cyanopindolol binding (250fmol/mg membrane protein) and rank order potency typical of the β_2 adrenergic receptor. Though the synthesis was reported as cell free, the system was designed in such a way that the final protein was still in the presence of a variety of other membrane bound proteins; a situation that is not ideal. More recently, Sansuk, et al (2008) have demonstrated cell-free production of the H_1 histamine receptor using the "RTS 500 ProteoMaster *Escherichia coli* HY" in vitro expression system from Roche. The receptor was expressed as a thioredoxin fusion protein and reached yields of 3 to 5 mg of receptor fusion protein per mL of reaction. These yields are substantial when compared with cell culture methods in chiwhc such quantities of protein may require litres of cells. Following IMAC purification (to

separate the receptor from other proteins required for translation) and reconstitution of the receptor into asolectin liposomes, assessment of the pharmacological properties of the receptor demonstrated it to be similar to a H_1R expressed using the baculovirus/insect cell expression system. A slightly decreased affinity of the *in vitro* produced H_1R was thought to be due to the absence of post translational modifications (which the *E.coli* extract can not perform). This work by Sansuk, et al., (2008) suggests *in vitro* cell free expression may well be a useful method for high yield expression of functional 7TMRs. This is an exciting prospect and well worthy of further research. Of particular interest may be the use of cell free expression systems which are able to perform post translational modifications or produce receptor in such a way that it does not require solubilisation prior to purification.

1.7. 7TMR Solubilisation

The amphiphilic nature of detergent molecules makes them an ideal midway between receptor removal from cell membrane to receptor reconstitution into a defined lipid environment. There are a large number of detergents available for membrane protein solubilisation and three examples are given in a Table 4. Detergents can be divided into three groups according to the hydrophilic head group found at the end of the hydrocarbon chain. Ionic detergents have a head group with a net charge, for example sodium cholate (also known as a bile acid salt). Non ionic detergents have uncharged head groups and these detergents are considered better suited to protein purification than ionic detergents as they tend to break lipid-lipid and lipid-protein interactions. Finally, zwitterionic detergents combine both ionic and non-ionic properties. Though zwitterionic detergents have no net charge they are effective in breaking protein-protein interactions. The critical micelle concentration (CMC) is defined as the concentration at which detergent monomers begin to arrange into micelles. The CMC is given as a range reflecting the nature of micellar formation. Increasing the number of double bonds in a detergent increases the CMC, as does the presence of counter ions in the case of ionic detergents. CMC will decrease with increasing alkyl chain length. In aqueous solutions, detergents have three phases; a crystal phase, a monomeric phase and a micellular phase. The detergent will be in one or all of these phases depending on concentration and temperature. As the temperature of the solution is increased, the detergent will move through the stages in the order given above, until the solution monomer concentration reaches the CMC at which point the detergent will principally be in the micellular phase. The temperature at which this occurs is the critical micellar temperature and the point of phase equilibrium is the Kraft point.

Table 4. The structure, type and CMC of 3 common detergents used in protein purification. Structures show the varying nature of head group type (ionic/non-ionic/zwitterionic).

Name	Structure and Type	CMC (mM)
Sodium Cholate	Ionic	9-15
Digitonin	Non-ionic	<0.5mM
CHAPS	Zwitterionic	5-6mM
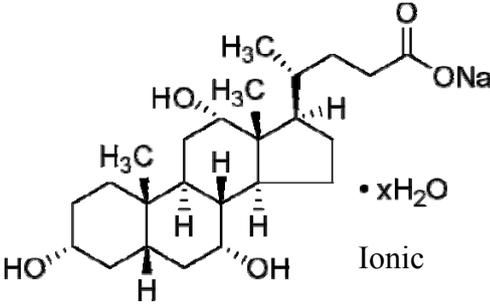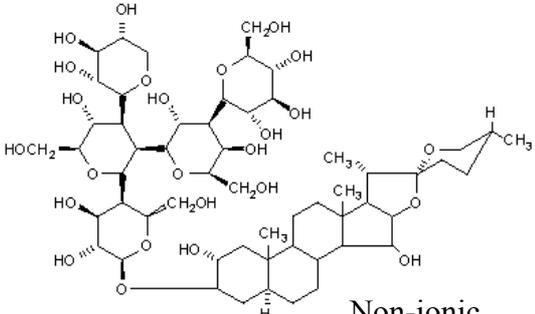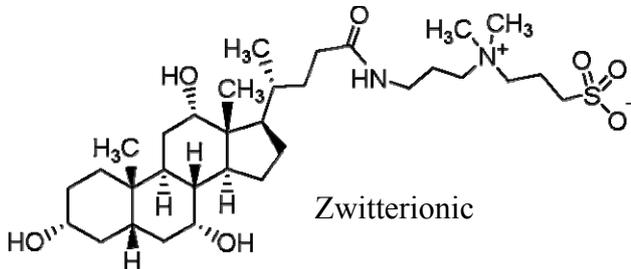
A single 7TMR may have several detergents reported as optimal for solubilisation of the receptor. The detergent used can vary with the cells used to express the receptor, but most importantly the detergent must be chosen to maximise effectiveness of receptor solubilisation in conjunction with maintenance of the receptor activity (generally the maintenance of the receptor's orthosteric binding site is classified as "active" receptor). Some considerations when purifying proteins may be the addition of stabilisers to the solubilisation buffer, which may include an appropriate ligand or glycerol.

1.7.1. Solubilisation of the M$_2$ Muscarinic Receptor

In early 7TMR work the muscarinic receptor was sourced from tissue. Florio and Sternweis, (1985) solubilised muscarinic receptor from bovine brain. In a method typical of the era, tissue was homogenised and membranes prepared through crude filtration. In this report the ionic detergent sodium deoxycholate (final concentration 0.75% w/v) was used. An important addition to the solubilisation buffer was the ligand atropine, which aids to stabilise the receptor. Ligand addition at the solubilisation step has proven to be useful in retaining functionality for a number of 7TMRs (Liitti, et al., 2001; Ratnala, et al., 2004). Another additive that was used in this report, and is commonly used in solubilisation protocols, was glycerol (20% w/v). When sodium deoxycholate was used an efficiency of approximately 75% recovery of 3-quinuclidinyl benzilate (QNB, a muscarinic ligand) binding sites was reported. Digitonin (2% w/v) has been used to solubilise muscarinic receptors from porcine brain, though only 28% of QNB binding activity was retained (Haga and Haga, 1983). Haga and Haga, (1983) showed that sucrose monolaurate was useful for muscarinic receptor solubilisation from porcine atrial membranes. A concentration of 0.3% (w/v) sucrose monolaurate combined with 1.2mg/mL membrane protein, effected a 50% solubilisation of [^{3}H]-QNB binding sites. Interestingly, 80% of [^{3}H]-N-methyl scopolamine (NMS) binding sites were retained suggesting structural instability of the solubilised receptors. The authors reported that CHAPSO (0.5%, similar to CHAPS but with an additional hydroxyl on the head group), digitonin (1% w/v) and digitonin/cholate (1% w/v, 0.1% w/v) were all less effective in muscarinic receptor solubilisation compared with sucrose monolaurate. However, sucrose monolaurate effected the solubilisation of 90% of total protein, as compared to 44% and 54% for digitonin and digitonin/cholate, respectively. In a thorough detergent screening process, Rinken, (1996) tested sixteen different detergents for solubilisation of muscarinic receptors from porcine atrial membranes. Of the sixteen, highest efficiency was achieved by digitonin (43% of QNB binding retained), sucrose monolaurate (55%) and digitonin/cholate (62% efficiency). It is important to note that in the case of the tissue solubilisations just reported it is difficult to distinguish which of the muscarinic receptor subtypes is being solubilised. Tissue sources may contain the full spectrum of muscarinic receptors and the paucity of subtype-specific ligands makes pharmacological characterisation difficult.

Rinken, et al., (1994) screened a variety of detergents for purification of all muscarinic receptor subtypes (M_{1-5}). Reflecting the challenge of 7TMR solubilisation/purification the researchers showed that even the subtypes within the muscarinic family (i.e M_{1-5}) required different solubilization conditions. A combination of sodium cholate (0.4% w/w) and digitonin (0.1% w/w) resulted in 63% recovery of the M_2 receptor from $Sf9$ insect cell membranes as defined by specific [^{3}H]-NMS binding. On the other hand, the zwitterionic CHAPS was shown to be ineffective in the solubilisation of muscarinic receptors. Whilst the non-ionic sucrose monolaurate (0.05 – 0.2%, w/w) solubilised 32% of scopolamine binding sites from membranes produced from M_2 infected insect cells. Furthermore, receptors solubilised with the digitonin/cholate mixture retained expected ligand binding affinities. Previously, Parker, et al., (1991) also showed that a combination of digitonin and cholate (1% and 0.2% w/v, respectively) solubilised up to 75% of QNB binding sites from infected $Sf9$ membranes. Additionally, after purification, the receptors were shown to have retained functionality by the ability to induce [^{35}S]-GTPγS binding to Gα$_o$. A digitonin/cholate mix appears to be the detergent of choice for M_2 solubilisation with Hayashi and Haga, (1996) also reporting its use (though solubilisation efficiencies were not given) for solubilisation from $Sf9$ insect cell membranes.

1.7.2. Solubilisation of the H_1 Histamine Receptor

H_1R has been solubilised from calf thymocyte membranes using nonidet-40 (1% w/v) and 300mM KCl (Osband and McCaffrey, 1979). The receptors were labelled with [^{3}H]-histamine prior to extraction from the membranes and subsequent chromatography. Toll and Snyder, (1982) determined digitonin (1% w/v) to be the most efficient and effective detergent concentration to solubilise H_1R from guinea-pig brain, as shown by [^{3}H]-doxepin binding. Digitonin (1% w/v) solubilised 50-75% of [^{3}H}-doxepin binding sites. Cholate, deoxycholate, tween-20, nonident-40, triton X-100 and octylglucose-pyranoside were also trialled with less success (Toll and Snyder, 1982). There is only one published example of solubilised H_1R from tissue-culture. Ratnala, et al., (2004) solubilised a Histidine tagged H_1R from $Sf9$ cells using 20mM DDM, this detergent treatment solubilised 40-50% of [^{3}H]-pyrilamine binding sites and proved the most efficient as compared to CHAPS and n-nonyl-β-D-glucoside (nG). Addition of 1M NaCl to the 20mM dodecyl maltoside (DDM) during solubilisation was reported to increase levels of H_1R solubilisation to 70-90%.

These three publications alone further demonstrate the irregular nature of 7TMR purification using detergents.

1.8. 7TMR Purification

There are a number of techniques available for membrane protein purification. Immuno-precipitation uses antibodies specific for a region on the 7TMR with the advantage that receptor subtypes can be separated from one another. The advent of commercially available antibodies to many 7TMRs has simplified this technique but it is still a long and expensive process. Attachment of a ligand to a resin allows for 7TMR separation by affinity chromatography. This was a common technique used with muscarinic receptors in early research where the ligand aminobenzhydryloxy-tropane (ABT) was used (see below). Again there are large time requirements in the preparation of the ligand (in the case of ABT, though commercial alternatives are now available) and subsequent attachment to a resin. A further disadvantage is that the captured receptor then requires elution with a competing ligand and if the receptor is to be used later in binding assays an additional step is required in order to remove the competing ligand used for elution. Alternatively, PCR can be used to attach a "tag" (an additional sequence at one end of the termini) to the protein sequence of interest. FLAG, c-Myc- and His are among the tags used with 7TMRs (Janssen, et al., 1995; Kobilka, 1995; Park and Wells, 2003; Park, et al., 2001). The concern with these techniques is that altered receptor structure may affect function. Cleaving the tag off after purification, by incorporation of a protease cleavage sequence into the receptor sequence construct, may help to rectify this. The localisation of negative charge associated with multiple Histidines may also lead to unexpected functional results (this was shown with rhodopsin) (Janssen, et al., 1995).

A classical antibody protein purification protocol is described by Liitti, et al., (2001), who used the technique to purify the α_{2C} adrenergic receptor. Receptor specific antibodies to part of the third intracellular loop were produced in mice and then coupled to a Sepharose column resin. Solubilised receptors were loaded onto the column and eluted with sodium thiocyanate (a chaotrope) with approximately 46% of the receptors being recovered (though ligand binding on lipid reconstitution was only 3.4%). Though purification was evident from SDS-PAGE results, the protocol was long and gave low overall recovery. A combination of receptor tagging and immuno-chromatography was used to purify the

CXCR4 7TMR (Babcock, et al., 2001). A C9 peptide sequence (from part of bovine rhodopsin) was introduced at the C terminus of CXCR4 allowing use of the corresponding C9 antibody (ID4) for purification. Though not the intent of Babcock, et al., (2001), a technique such as this may be useful if commercially available antibody is not readily available for the receptor of interest.

Haga and Haga, (1983) coupled ABT to epoxy activated sepharose to produce a gel capable of binding muscarinic receptors with a K_d of 7nM for the interaction. 70% of QNB binding sites were immobilised on the resin with subsequent elution resulting in 25% recovery. This large decrease in recovery was, at the time of publication, inexplicable, also the protein concentration was too low to be accurately determined yet SDS-PAGE analysis showed the presence of several bands. The authors did however suggest a 1000-fold purification. Haga went on to improve protein recovery achieving 74% recovery of muscarinic receptors from solubilised porcine atrial membranes (Rinken and Haga, 1993).

Histidine tagging has been used with a variety of 7TMRs with successful results (Janssen, et al., 1995; Kobilka, 1995; Ratnala, et al., 2004). A hexa-Histidine tag has been added to the C terminus of (bovine) rhodopsin (Janssen, et al., 1995). The His- tagged receptor was produced in *Sf9* insect cells and purified from membranes using immobilised metal affinity chromatography (IMAC). The authors reported a 500-fold purification to a level of approximately 70% which was aided by recovery of about 85% of receptors (determined from SDS-PAGE and UV/Vis spectroscopy). A combination of His- and FLAG tagging allowed for a nearly 100% pure β_2 Adrenergic receptor (C terminal His, N terminal FLAG) purification from *Sf9* insect cells (Kobilka, 1995). Although there was low specific dihydroalprenolol binding (6nmol/mg), suggesting that few of the purified receptors were functional.

1.8.1. IMAC Purification of the M_2 Muscarinic Receptor

Histidine residues have previously been attached to the C terminal of human M_2R sequence (Hayashi and Haga, 1996). Incorporation of this constructed gene into a baculovirus allowed for infection of *Sf9* insect cells and subsequent membrane preparation. Using immobilised metal affinity chromatography, 40% of receptors were recovered. The authors noted that in their system, cobalt loaded resin was more effective at retaining the

His- tagged protein than the commonly used nickel. Strangely, SDS-PAGE analysis of proteins prepared in this way showed two bands of approximately half the expected size of the receptor. Though the purification protocols used would suggest that these bands represent the M_2 receptor, the authors do not give an explanation for the smaller than expected product size. Additionally, although carbachol stimulated [^{35}S]-GTPγS binding was shown for M_2R purified by ABT-Sepharose, it was not shown for Histidine tagged receptors purified by IMAC perhaps reflecting structural/functional problems associated with adding such a sequence to the receptor. Finally, there does not appear to be any published examples of a His- tagged M_2 purified receptor being functionally recombined with G-proteins (i.e. agonist stimulated GTP binding).

1.8.2. IMAC Purification of the H_1 Histamine Receptor

A single method has been published for purification of a Histidine tagged H_1R (Ratnala, et al., 2004). Using nickel charged resin, a purity of 75-95% H_1R was obtained. Contaminants could be removed by washing with 20mM imidazole and the deca-Histidine tagged H_1R began to elute at 100mM imidazole, as shown by dot blot analysis using an anti-Histidine antibody. The radiolabelled H_1R inverse agonist [^{3}H]-mepyramine (also known as [^{3}H]-pyrilamine) was incorporated throughout the small scale purification protocol (whilst tripelennamine was used in larger scale purifications) and a final value of 58% recovery of functional receptor was stated. Encouraging is that at least part of the purified receptor population retained similar affinities to the unpurified H_1R for a variety of ligands.

1.9.   Protein Crystallisation

A 3 dimensional (3D) crystal consists of a regularly ordered repeating pattern of atoms, the unit cell, which extends in three dimensions (Figure 8).
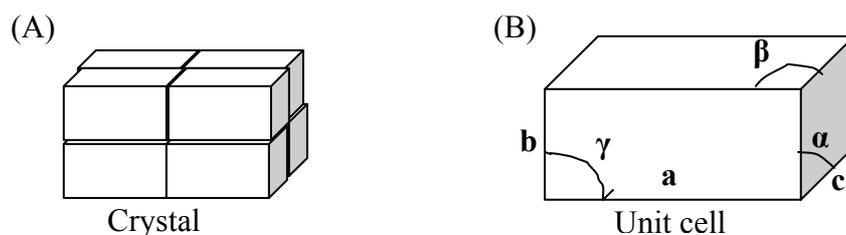
Figure 8. The crystal (A) is made from a repeating arrangement, the unit cell (B). The unit cell can not be broken down to a smaller, repeating arrangement. The unit cell is defined by three lengths (a, b, c) and three angles (α, β, γ).

Unit cells are classified by the lengths of **a**,**b**,**c** and the angles α, β, γ. For example, if **a** ≠ **b** ≠ **c**, α = γ = 90° and β > 90° the unit cell is termed monoclinic. There are 7 possible unit cell classes and 14 possible lattices (Rhodes, 2000). There are several sets of planes in a unit cell, the simplest of which are those described by the faces of the crystal. Figure 9 shows two different planes for a cubic unit cell, one parallel with a face of the cube (A) and another set angled to the face of the cube (B).
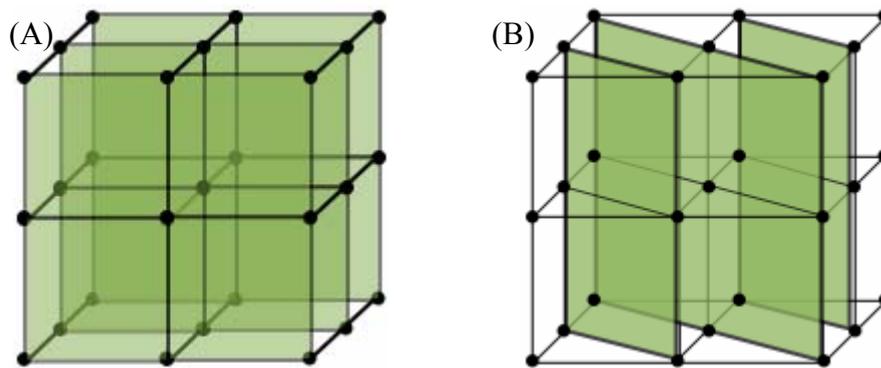
Figure 9. Planes in a cubic unit cell. (A) The (001) plane of a cubic unit cell. (B) The (023) plane of a cubic unit cell.

The planes of the unit cell are described by the indices *h*,*k* and *l*. The indice *h* describes the number of planes in the x direction of the unit cell, *k* is the number in the y direction and *l* in the z direction. Alternatively the indices can be described as the number of parts the set of planes cut the **a** (*h* indice), **b** (*k*) and **c** (*l*) edges of the cell.

To produce a protein crystal requires a super-saturation of the protein suspension to the point that non-covalent interactions hold the proteins together in an ordered arrangement – the crystal. The crystalline state can be achieved by slowly lowering the solubility of the protein in an attempt to promote nucleation, the initial point from which a crystal can grow. Nucleation begins when the protein starts to form nanometre sized clusters. Not all clusters will be stable and the protein clusters may re-disperse. At some point the protein cluster reaches a size that is stable (dependent on crystallisation conditions) and it is at this point that the crystal structure is defined. Crystal growth and nucleation continue whilst the protein remains in a supersaturated state. Protein super-saturation is most commonly achieved by vapour diffusion (see section 1.9.1) and this method has been successful for a large number (around 40,000 in the protein database) and variety of proteins, the majority

of which are not integral membrane proteins. Integral membrane proteins, with their hydrophilic and hydrophobic domains, have presented a challenge. Recent success has been achieved using *in meso* (or *in cubo*) three dimensional crystallisation (Cherezov, et al., 2007; Rasmussen, et al., 2007).

The alternative to 3D crystallisation is crystallisation of the protein in only two dimensions (2D crystallisation). In simple terms 2D crystallisation is the reconstitution of the protein into a lipid bilayer in such a way that the protein is ordered along the vertical and horizontal planes of the bilayer. Crystals are visualised by electron microscopy and analysed by electron diffraction. The technique has somewhat fallen out of favour due to the rapidity in which structural information can be gained using x-ray diffraction of 3D crystals as opposed to the very long times required for the generation of projection maps by electron microscopy/diffraction. However, like *in meso* 3D crystallisation, 2D crystallisation provides an ideal environment for crystallising membrane proteins.

1.9.1. Vapour diffusion 3D crystallisation of membrane proteins

Protein crystallisation is most commonly achieved by vapour diffusion (Figure 10).
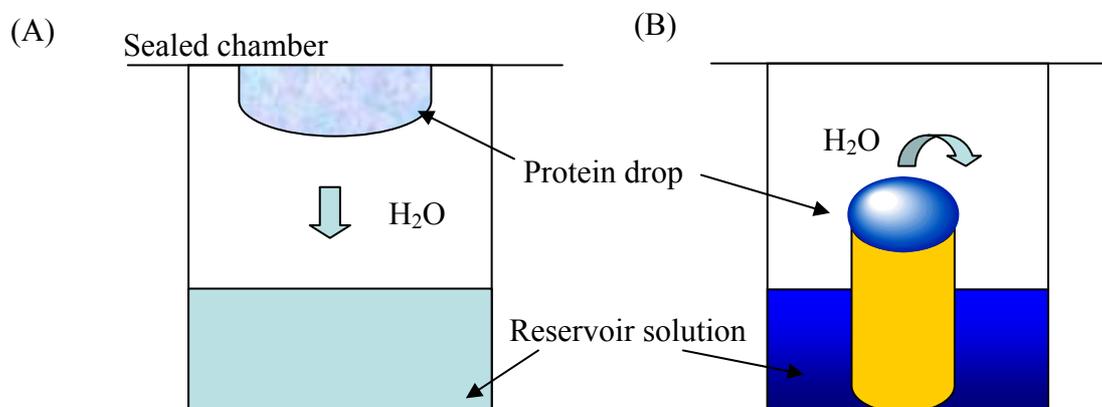
Figure 10. The vapor diffusion technique for protein crystallisation. (A) Hanging drop vapour diffusion, water transfer occurs from the less concentrated protein drop to the more concentrated reservoir solution. (B) Sitting drop vapor diffusion.

The protein is combined with a "reservoir solution" and a drop of this protein suspension is placed in a chamber containing a higher concentration of the reservoir solution. The reservoir solution is made up of one or more of a buffer, salt and a precipitating reagent. Since the reservoir solution is more concentrated than that in the protein drop, water transfer (diffusion) occurs from the protein drop to the reservoir solution. This gradually

increases the concentration of the protein (and other reservoir solution reagents) in the drop. Experimentally, vapour diffusion can be achieved by the hanging drop (Figure 10A), sitting drop (Figure 10B) and sandwich drop methods. Vapour diffusion methods are standard practise for soluble proteins and automated, high-throughput crystallisation trials are common to many laboratories. Vapour diffusion methods have been less successful for membrane proteins but are not without exception. Most notably the photosynthetic reaction centre was crystallised using vapour diffusion and the protein structure was solved to a resolution of 3Å (Deisenhofer, et al., 1985).

1.9.2. *In meso* 3D crystallisation of membrane proteins

Another method which presumably provides a basis for slow concentration of the protein to be crystallised is *in meso* (also known as *in cubo* crystallisation, *in meso* is used here since the meso phase covers the variety of cubic structures of the surfactant which can be formed) (Caffrey, 2003). In between the highly ordered solid and the disordered liquid state, surfactants spontaneously arrange into a variety of semi-ordered structures that constitute the surfactant mesophase (Figure 11) (Caffrey, 2003).

.

Lamellar crystal - Lc   Lamellar liquid crystal - L$_\alpha$
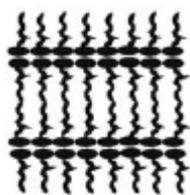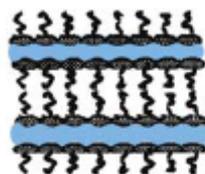
Cubic - Pn3m   Cubic - Ia3d
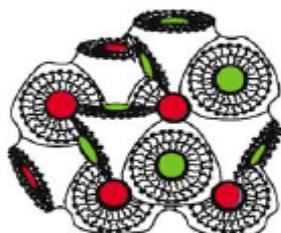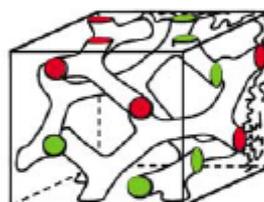
Cubic - Im3m   Inverted hexagonal - H$_{II}$
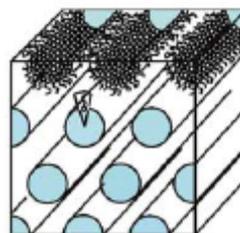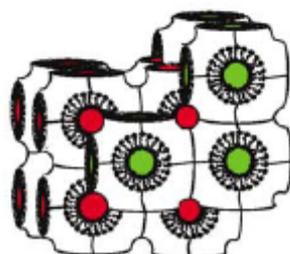
Figure 11. Surfactant structures in the mesophase (Caffrey, 2003). Structure formation is spontaneous in an aqueous environment due to the amphiphilic nature of the surfactant and the hydrophobic effect. Properties of the structure are determined by surfactant structure, temperature, pressure, water concentration and the presence of additives (salts etc.).

The properties of the surfactant arrangements are determined by structure of the surfactant, temperature, water content and pressure. The movement between structures (phases) is described by the phase diagram. The structure and phase diagram for the surfactant monoolein is shown in Figure 12 (Qiu and Caffrey, 2000). Clearly for use in protein crystallisation the choice of surfactant will depend at least in part on the conditions under which mesophase structures are formed. For this reason, monoolein is well suited to *in meso* protein crystallography due to cubic phase (Ia3d, Pn3m) formation at temperatures compatible with the retention of functional protein (e.g. 20°C, 40% water content, see Figure 12). To date, monoolein has been the only surfactant to have been used in published examples of *in meso* protein crystallography. There are several other surfactants which would be compatible with protein crystallisation, such as phytantriol (Barakaus and Landh, 2003) and others currently being investigated by CSIRO Chemistry, Clayton.
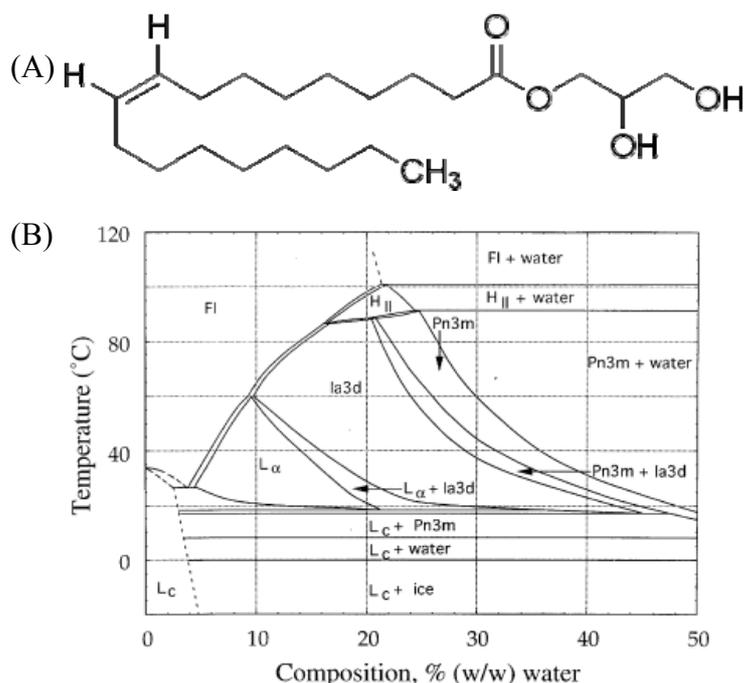
Figure 12. (A) Structure of monoolein, a typical surfactant. (B) Phase diagram of monoolein showing structure transitions within the mesophase, as determined by small angle X-ray scattering (SAXS) (Qiu and Caffrey, 2000). Abbreviations are defined in Figure 11, with the exception of F1, which represents the fluid isotropic phase.

In meso crystallisation involves mechanical mixing of a detergent solubilised protein suspension with the lipid surfactant, with the protein suspension providing the aqueous component for cubic phase formation. For membrane proteins, the lipid bilayer of the *in meso* phase provides an environment for reconstitution of the hydrophobic regions of the protein. The addition of salts to the surfactant/protein mixture can induce crystal formation. As water is withdrawn by the salt, the cubic phase contracts, potentially concentrating the now lipid reconstituted protein. Concurrently the increase in ionic strength may also facilitate protein-protein interaction. Electron, atomic force microscope and microbeam X-ray studies have suggested the presence of a lamellar phase between the cubic phase and protein crystal (Cherezov and Caffrey, 2007; Paas, et al., 2003; Qutub, et al., 2004), suggesting that a lipidic phase transition may be important in formation of the protein crystal. Cubic phase crystallisation has been used for crystal production and structure determination of lysozyme (Landau, et al., 1997), rhodopsin II transducer complex (Gordeliy, et al., 2002) bacteriorhodopsin (Luecke, et al., 1998) and, in two ground breaking publications, two different forms of the β_2-adrenergic receptor as discussed in section 1.10.4 (Cherezov, et al., 2007; Rasmussen, et al., 2007).

1.9.3. 2D Crystallisation of Membrane Proteins

Formation of two dimensional (2D) crystals involves purification of the protein of interest (including detergent solubilisation) followed by removal of detergent and concurrent reconstitution into a lipid bilayer (Figure 13). As detergent is removed from the mixture, the protein interacts with the lipids in order to protect the hydrophobic portions of the protein from the surrounding aqueous medium (Levy, et al., 2001; Rigaud, et al., 2000). A combination of protein and lipid dependant factors then determine whether the protein packs in a crystalline manner in the lipid bilayer. These factors include the lipid to protein ratio (LPR), temperature, the presence of salts and lipid structure (Tsai, et al., 2007).

Protein of interest

Membrane solubilisation and protein purification

Detergent removal
Lipid addition

Protein in detergent micelle

Protein packing in lipid bilayer
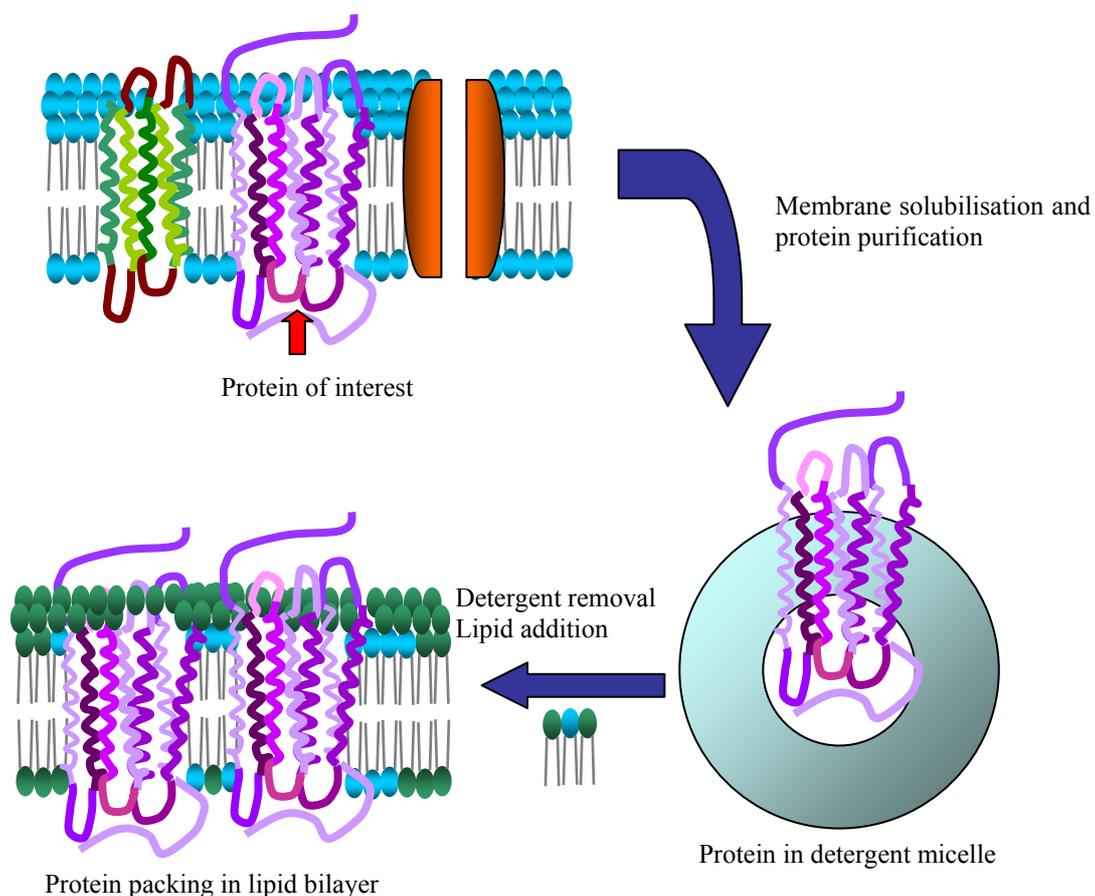
Figure 13. Schematic of 2D crystallisation process for membrane proteins. In most cases the protein of interest must be solubilised using detergents and purified from contaminating proteins. Lipids are added to the purified protein/detergent micelle complex and the detergent is concurrently removed. Detergent removal prompts protein reconstitution into the lipid bilayer and, ideally, packing of the protein into an ordered array.

Generally for crystalline packing of the protein in the lipid, a high protein to lipid ratio is required. The actual ratio of protein to lipid may vary from that theoretically calculated depending on the aggregation of the protein suspension since aggregated protein may be

less available for crystallisation (Hasler, et al., 1998). 2D crystals may take multiple arrangements as shown in Figure 14 (Rigaud, et al., 2000).
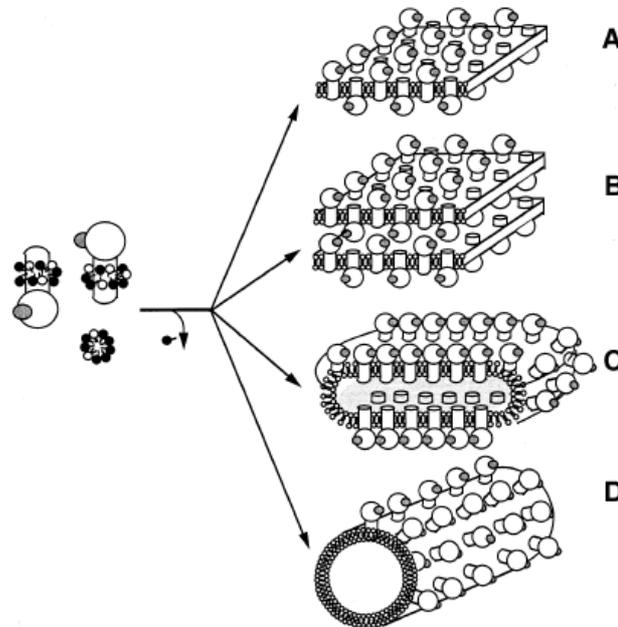
Figure 14. 2D protein crystals can form multiple arrangements. Image reproduced from (Rigaud, et al., 2000). (A) planar crystal, (B) layered planar crystals, (C) vesicular crystals and (D) tubular crystals.

There are a number of issues to be considered when deciding on an appropriate lipid combination and experimental set up for 2D crystallisation. However, since the exact mechanisms of 2D crystal formation are unknown and will vary between proteins, the choice of conditions is somewhat a trial and error process. A single protein may form 2D crystals under multiple conditions (Rigaud, et al., 2000). Clues can be taken from prior published 2D crystallisation methods (not available for M_2R or H_1R) or publications using lipid reconstitution for other purposes such as purified protein activity. Factors to consider include, lipid structure, lipid transition temperature (and thus temperature at which the 2D crystallisation experiment is carried out), buffer composition, detergent removal method and the lipid to protein ratio used.

Lipids may be either derived from tissue or produced synthetically. Due to issues of stability and contamination, synthetic lipids are generally superior than their tissue based counter parts. Synthetic lipids can suffer from stereochemical impurities (due to synthesis from glycerol). For lipid preparations to be used in aqueous formulation, incorporation of cholesterol or carbohydrate into the lipid mixture may aid to stabilise the lipids from

hydrolysis. The phase transition temperature of the lipid will vary with saturation (double bonds decrease the transition temperature), hydrocarbon length (an increase in length correlates with an increase in phase transition temperature – due to stronger van der Waals interaction), species of lipid headgroup, and charge. In most cases a mixture of lipids is required to provide properties suitable for the protein. For example, addition of cholesterol can be used to manipulate the membrane fluidity with cholesterol playing the role of "filling in the gaps" of imperfectly packed lipids. The large variety of expression systems used with 7TMRs, suggests that integral membrane proteins are suited to a wide range of lipid environments.

After addition of lipid to the protein/detergent micelles, the detergent must be removed forcing the protein to interact with the lipids (and ideally causing the proteins to interact with each other and pack into a 2D crystal). The two most common methods of detergent removal for 2D crystallisation experiments are dialysis and the use of detergent absorbants such as bio-beads (BioRad) (Daniels, et al., 1999; Jahn, et al., 2001; Rigaud, et al., 1997; Unger, et al., 1999). Dialysis can be carried out in commercially available microdialysis devices suitable for the small volumes of protein used in crystallisation set up. For detergents with a CMC greater than about 5mM, dialysis is a relatively fast method for detergent removal. Dialysis has been successfully used to remove dodecyl-β-D-maltoside (CMC ~0.15mM) for 2D crystallisation of lactose permease (Zhuang, et al., 1999), and for removal of CHAPS for crystallisation of the mannitol transporter transmembrane domain (Koning, et al., 1999). Bio-beads are able to rapidly remove detergent regardless of CMC (Rigaud, et al., 1997). Additionally varying the amount of beads can be used to control the speed with which detergent is removed. It may however suffer from the disadvantage of loss of protein if the beads are not carefully used (Rigaud, et al., 1995). A different approach for detergent removal makes use of cyclodextrin inclusion compounds, though this technique was not inititally designed for 2D crystal formation (Degrip, et al., 1998). The authors utilised this method for lipid reconstitution of the H_1R (followed by NMR studies) (Ratnala, et al., 2004). Cyclodextrins selectively sequester detergent molecules whilst having low binding affinities for (diacyl)phospholipids. The authors propose a mechanism in which the cyclodextrin/detergent complex is formed by inclusion of the detergent's hydrophobic tale into the cavity of the cyclodextrin. Cyclodextrin compounds were added stepwise to a protein/detergent/lipid mix, the mixture was then separated by centrifugation using a sucrose gradient with the proteoliposome resolved in the 20% layer.

Residual detergent could be analysed by Fourier Transform infrared spectroscopy (FT-IR). Using FT-IR it was confirmed that fewer than 1 cyclodextrin molecule and 3-4 detergent molecules in 40 phospholipids (FT-IR detection limit) could be detected, suggesting this to be a useful method for detergent removal which may not suffer from high protein yield loss (reported protein recovery was between 70 and 90%).

Following detergent removal, which may take between hours and days, the proteo-lioposomes are prepared for electron microscopy and analysed for the presence of 2D crystals. Examples of 2D crystals are given in Figure 15.
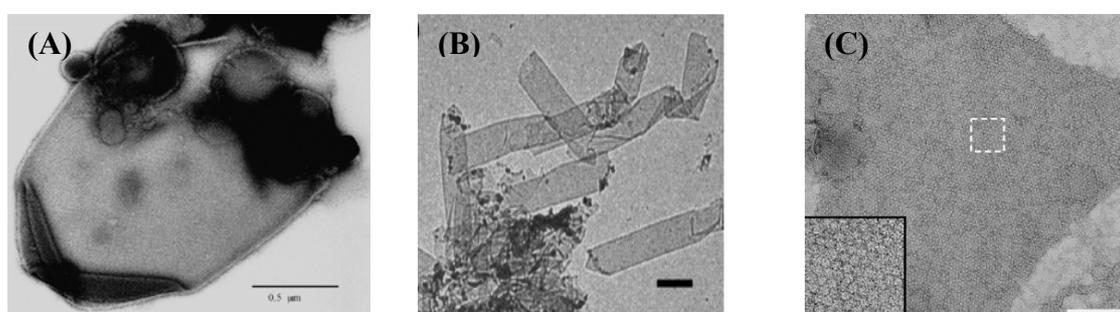
Figure 15. Examples of 2D crystals viewed by electron microscopy. (A) Recombinant ATPase 2D crystal (Jahn, et al., 2001). (B) Tubular 2D crystals of glycine-betaine transporter (Tsai, et al., 2007). (C) Mitochondrial ATP synthase crystal (Arechaga and Fotiadis., 2007) All crystals are negative stained with uranyl acetate.

An alternative method to concurrent lipid addition and detergent removal for 2D crystallisation is the "2D crystallisation on lipid layer" technique (Levy, et al., 1999; Rigaud, et al., 2000). In this method a film of functionalised lipid is formed at an air water interface. The protein is added and interacts with the functional group on the ligand (i.e. the functionalisation of the lipid is used to couple a ligand to the protein of interest onto the lipid molecule). This is followed by self organisation of the protein/lipid array into 2D crystals. The technique is useful for soluble proteins but has also been used successfully with integral membrane proteins (Arechaga and Fotiadis, 2007).

Bayburt and Sligar, (2003) developed a technique for producing discoidal, nanoscale phospholipid bilayers. (Bayburt and Sligar, 2003; Civjan, et al., 2003; Denisov, et al., 2004) Amphipathic membrane scaffold proteins (MSPs) were engineered and combined with phospholipids and detergent. When the detergent is removed, a self assembly process is initiated in which "nanodiscs" are formed (Figure 16). Forming a ring-like structure

around the phospholipids, the α helical proteins serve the purpose of protecting the hydrophobic portions of the lipids from an aqueous environment. Bacteriorhodopsin (a 7TMR) was reconstituted into the nano-discs with high efficiency (around 93%) and all-*trans*-retinal binding showed a dissociation constant similar to that measured in purple membrane.
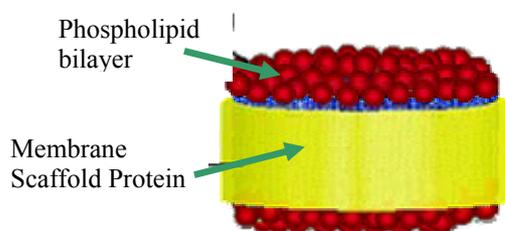
Figure 16. Schematic of a nanodisc formed following detergent removal from a detergent, scaffold protein, lipid mixture. Image reproduced from (Bayburt and Sligar, 2003).

Discs containing the receptor where analysed by atomic force microscopy and shown to be ~10nm in diameter, corresponding well with the incorporation of a single bacteriorhodopsin receptor and further confirmed using circular dichroism (Bayburt and Sligar, 2003). Lipid discs containing a single β_2 adrenergic receptor have also been produced and the receptor has retained the ability to interact with $G\alpha_s$ prompting the authors to suggest that oligomirisation of the receptor is not required for activation of G proteins (Service, 2004; Whorton, et al., 2007). The ability to direct a single protein into a lipid bilayer may provide a unique method for 2D crystal formation, or indeed 3D crystallisation. Furthermore, the scaffold proteins could be engineered to contain useful sequences, for example a repeating Histidine sequence, which could be used to anchor the discs to a surface.

1.10. Protein Crystallography

1.10.1.   Diffraction

Diffraction is the result of interference of waves. For example, waves which emanate from two narrow slits (a diffraction grating) will interfere with each other (Figure 17). Interference is constructive when the two waves are effectively superimposed on each other i.e. the two waves are in phase with each other, resulting in greater total amplitude. Destructive interference occurs when the waves are out of phase and so the total amplitude is decreased. Taken together, constructive and destructive interference lead to regions where there is no wave and regions where the wave is amplified (i.e. diffraction spots).
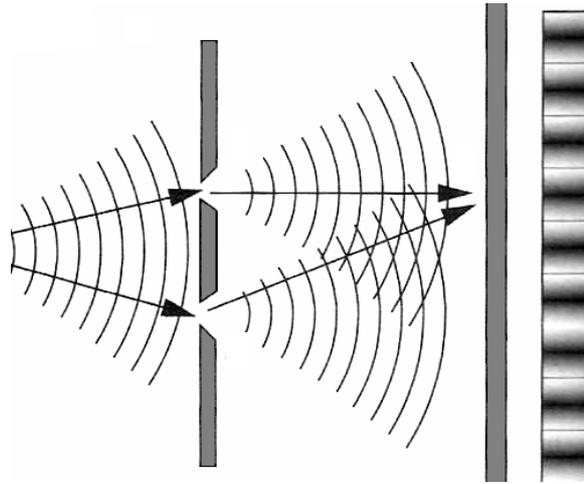
Figure 17. Diffraction of a wave by two slits of a diffraction grating. After passing through the slits, the emanating waves will either constructively of destructively interfere with each other resulting in regions of increased wave amplitude and regions of no wave amplitude (no wave).

A crystal is a diffraction grating. The periodic structure of the crystal causes a particular type of interference, since the waves are reflecting from the different crystal planes. Interference of a wave from the planes of a crystal is known as Bragg diffraction and it was first described by investigation of X-rays with crystals.

1.10.2.   X-Ray diffraction for Protein Crystallography

The Australian father and son duo William Henry Bragg and William Lawrence Bragg were amongst the first to investigate the interaction of X-rays with matter. In fact the first medical use of X-rays in Australia was performed by William Henry on his son's arm after William Lawrence fell from his bicycle (Wikipedia, 2007). It was William Lawrence who first described the relationship between the X-rays that are directed at a crystal and those that emerge from the crystal. As an X-ray beam hits a crystal, the X-rays are elastically scattered/diffracted by electrons in the atoms making up the crystal. The scattered X-rays are recorded as a series of spots (reflections) giving rise to a distinct diffraction pattern. Each reflection in the diffraction pattern represents constructively interfering X-rays diffracted from a plane of the crystal's unit cell. A complete diffraction pattern can be obtained from one unit cell, the fact that the crystal is comprised of repeating unit cells means that not only does the crystal act as a diffraction grating but it also amplifies the diffraction signal. By treating diffraction of the X-ray (or other wave) as a reflection from

sets of equivalent, parallel planes of atoms in the crystal, Bragg demonstrated that it was possible to calculate the angles at which the diffracted beams would emerge, as described by Bragg's law (Equation 1).

$$2d_{hkl} \sin\theta = n\lambda$$

Equation 1. Bragg's law of diffraction. Where d is the interplanar spacing, *hkl* is the index of the parallel planes, n is an integer, λ is the wavelength of the X-rays and θ is the angle at which the X-rays hit the planes of the crystal.

Bragg diffraction can only be observed under conditions in which n is an integer. At fractional values of λ, deconstructive interference occurs between the diffracted X-rays. Taking into consideration wave-particle duality and the associated deBroglie wavelength, it follows that this description of diffraction is not limited to X-rays but can also describe neutron and electron diffraction. An alternative but complementary way of analysing diffraction is to treat each atom, or electron dense area, as an independent diffractor. Each reflection (emerging X-rays) is described by a Fourier series made of terms representative of each atom in the crystal. A detailed explanation of Fourier analysis has been written by (Rhodes, 2000). A combination of Bragg and Fourier analysis of the diffraction pattern from the crystal provides nearly all the information required to calculate an electron density map of the unit cell. The final piece of information required is the phase for each reflection in the diffraction pattern. Phases can be determined by molecular replacement, multiwavelength anomalous diffraction (MAD) or heavy atom soaking (Rhodes, 2000). Bragg and Fourier analysis in combination with a method for phase determination, allows calculation of the electron density map for the unit cell of the crystal. In the case of a protein crystal, the unit cell electron density represents structure of the protein itself.

1.10.3.   Production and Detection of X-rays for Crystallography

X-rays for crystallography are produced by directing high energy electrons onto a metal target, most commonly copper or molybdenum. The high energy electrons are produced by a heated filament and accelerated by an electric field into a rotating, cooled metal target (anode). If these high energy electrons knock out an electron in the lower energy orbitals (e.g. K shell) of the metal target, X-rays are produced by the decaying of an electron from a higher orbital (e.g. L shell). For example, copper can undergo two transitions when electrons from the K shell are removed. The L to K transition emits X-rays of 1.54Å in

wavelength while the M to K transition produces X-rays of 1.39Å in wavelength. For analysis of the diffraction pattern, a monochromatic starting source is required (polychromatic sources make the calculations near impossible). For this reason a second metal is used as a filter for the lower energy (M to K transition) X-rays. For copper, this second metal would have an absorption wavelength equal to 1.39Å and thus would filter the M to K transition energy. After passing through the filter the monochromatic X-rays are reflected into a narrow beam (collimation) and mirrors are used to focus the beam onto the crystal. Production of X-rays is extremely inefficient, with much of the energy being lost as heat. Cooling systems are required to maintain the X-ray system at a low temperature enabling X-rays to be continually produced. X-rays can also be produced from synchrotron radiation. In this case after being produced by filament heating, the electrons are accelerated around a ring (the circumference of which is in the range of 400 – 1000 metres) at speeds near that of light. Magnets, oscillators, modulators and wigglers are used to direct the electrons. Focusing mirrors and monochromators direct high energy X-rays into beamlines coming off of the storage ring.

Image plates are the most common method of detecting diffracted X-rays. The plates consist of phosphor coated plastic sheets. $BaF-Eu^{++}$ is a commonly used phosphor. Incident X-rays stimulate electron transfer from Eu^{++} to F^-. Following X-ray exposure, a laser scans the image plate causing decay of the electron back to the Europium layer, the visible light released from this decay is proportional to the intensity of the original diffracted X-ray beam. The emitted visible light is recorded by a photocell and reported to a computer for processing into a diffraction image.

1.10.4.   X-ray Crystallography of 7TMRs

One (near) complete (Palczewski, et al., 2000) and two partial structures (Cherezov, et al., 2007; Rasmussen, et al., 2007) have been solved by X-ray crystallography from three dimensional 7TMR crystals. A 2.8Å resolution structure of bovine rhodopsin was published in 2000, from crystals produced by hanging drop vapour diffusion of mixed micelles (Okada, et al., 2000). The crystals formed were long, narrow, purple and predominantly twinned (Okada, et al., 2000; Palczewski, et al., 2000). The structure gave interesting insights into 7TMRs. For example, the amino terminus was shown to extend to a beta sheet running parallel to the membrane. The second extracellular loop appeared to fold into the centre of the rhodopsin molecule. The helical bundle was shown to be

symmetrical along the perpendicular axis of the membrane with both faces of the bundle being equal in size. This is in contrast to the interpretation of molecular structure obtained using data from cryo-electron microscopy of 9Å resolution (Unger, et al., 1997). The preliminary (Palczewski, et al., 2000) structure showed 333 of the 348 amino acids of opsin. Several structures of bovine rhodopsin have since been released, reaching a resolution of 2.2Å in a study in which crystal growth conditions were modified to reduce twinning (Okada, et al., 2004). *In meso* reconstitution has been used to demonstrate the ability of the rhodopsin to activate its G-protein (transducin) in the cubic phase (Navarro, et al., 2002). This work may prove particularly useful if extended to other 7TMRs as the ability to couple 7TMR to Gα in the cubic phase may provide some stability to the flexible third intracellular loop and so aid in the crystallisation step.

In 2007 the partial structure of human β_2 adrenergic receptor (β_2R) was solved by two different groups, using two different receptor constructs (Cherezov, et al., 2007; Rasmussen, et al., 2007). Rasmussen, et al., (2007) used purified β_2R for the production of monoclonal antibodies in mice and subsequently produced antibody fragments (Fabs). A complex of inverse agonist (carazolol), β_2R (minus 48 amino acids on the C terminus) and Fab was reconstituted into 1,2-Dimyristoyl-sn-Glycero-3-Phosphocholine (DMPC) bicelles. Addition of ammonium sulphate as a precipitant was followed by growth of long, thin crystals which were believed to be stacks of two-dimensional crystals. A 3.4Å resolution structure was achieved for the transmembrane helical bundle, however high resolution information could not be gained for the N terminus, extracellular loops, part of the third intracellular loop and the C terminus.

Cherezov, et al., (2007) replaced the third intracellular loop of β_2R with the sequence for T4 lysozyme, a readily crystallizing protein. Crystals were produced by *in meso* crystallisation, β_2R was reconstituted with monoolein in the presence of 8-10% (w/w) cholesterol, 30-35% (w/v) PEG-400, 0.1-0.2M sodium sulfate, 0.1M Bis-tris propane pH6.5-7.0 and 5-7% (v/v) 1,4-butanediol. Incorporation of cholesterol improved crystal quality and was shown, like 1,4-butanediol, to be directly involved in the ordering which promoted the only interaction between symmetry-related receptors. Like the crystals described by (Rasmussen, et al., 2007), β_2R-T4 crystals consisted of multilayered protein arrays – essentially the stacking of sheets of the arrayed protein. Three of the four interactions holding the protein sheets together were determined to be between the T4

sequences, the fourth was receptor-receptor interaction mediated by the cholesterol and the alcohol as described above. Interaction between the sheets of protein is between the T4 sequence and the second and third intracellular loops of the β_2R. In total, only 27% of the contacts in the crystal were due to protein-protein interaction the remainder being due to ordered lipid molecules. A 2.4Å resolution structure was achieved for the transmembrane helices, resolution decreased to between 4 and 6.5Å for the extracellular and intracellular loops; amino acids 1-28 of the N terminus were not included in the structure, nor were amino acids 343-365 of the C terminus.

Both structures of the β_2R were determined by the molecular replacement method, either using regions of the Fab or the T4 sequence and poly-Alanine models of rhodopsin. Further, both groups suggested a requirement for a micro-focused X-ray beam (5-10μm) in order to measure reflections of the weakly diffracting crystals. Whilst Rasmussen, et al., (2007) obtained a complete data set from a single crystal, Cherezov, et al., (2007) used 27 crystals to obtain a complete data set.

The β_2R structures demonstrate that structure determination of such difficult proteins is achievable. However a significant amount of work has led to structure determination and the β_2R is relatively easy to express and manipulate in functional form compared to other type I 7TMRs (Day, et al., 2007; Granier, et al., 2007; Kobilka, 1990; Rasmussen, et al., 2007; Warne, et al., 2003; Whorton, et al., 2007; Yao and Kobilka, 2005; Yao, et al., 2006). Furthermore, neither structure is complete and perhaps more importantly for future work in this area, both structures relied on interaction of secondary proteins to produce crystals.

1.10.5.   Electron Diffraction for Protein Crystallography

Electron diffraction can be performed using a transmission electron microscope (TEM, Figure 18). In the TEM, electrons are produced by heating of a tungsten filament then focused by electromagnetic lenses onto an appropriately prepared sample, the emerging electron beam is magnified and the final image recorded either on a phosphor screen or by a CCD camera.
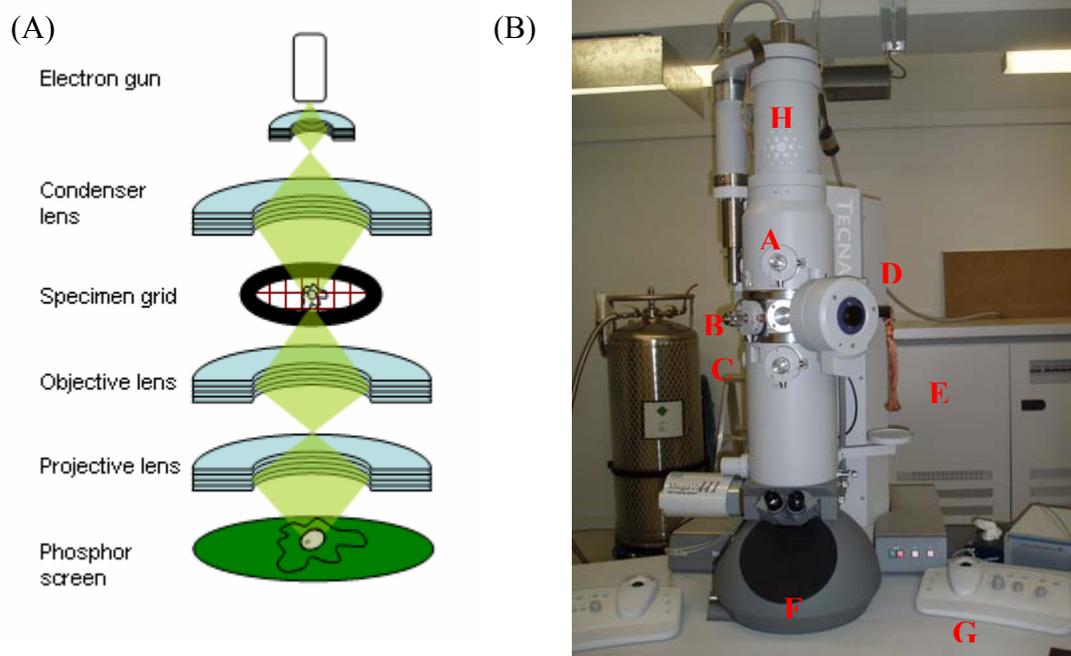
Figure 18. Transmission Electron Microscope. (A) Schematic of the internal part of a TEM. Electrons are produced at the top of the column by heating of a filament (electron gun), electric fields focus the electron beam through a condenser lens which further focuses the beam onto the specimen. Magnification of the image is achieved by the objective and projective lenses. A phosphor screen records the image. (B) Technai 12 Transmission Electron Microscope at CSIRO Molecular and Health Technologies Parkville. A - condensor lens; B - objective lens; C - projective lens; D - sample chamber; E - liquid nitrogen cooling copper tail; F - viewing window; G - controller pad; H - electron gun.

There are several methods for preparing samples for electron microscopy including dehydration, conductive coating, staining and cryo-fixation, the latter two will be described here. For both preparation techniques the sample is first absorbed to an electron microscopy 'grid'. The grid is made from one of a number of metals including nickel, gold or most commonly copper. The grids have a diameter of around 3mm and consist of a thin mesh of the metal, the mesh is most commonly hexagonal. A carbon film is layered on the grid and the sample is adsorbed to the carbon coated grid. Sample thickness should be <500nm in order to be electron transparent. Samples for electron microscopy are negatively stained using heavy metal compounds such as the commonly used uranyl acetate. Such heavy (negative) atom stains will accumulate around the biological sample and stain accessible areas within the sample but do not overly accumulate on the sample itself. The heavy atom scatter electrons, whilst biological samples tend to be weak scatters, thus electron microscopy of a negatively stained sample will produce an image of the stained areas from which the sample image can be inferred. For cryo-EM, samples are

adsorbed onto the grid and then rapidly frozen in either liquid ethane or liquid nitrogen. Rapid freezing of a hydrated sample causes formation of amorphous ice in which the water molecules are randomly arranged in a non-crystalline glass structure which covers the sample. The layer of ice preserves the specimen and the low temperature, (the sample chamber in the electron microscope is also maintained at liquid nitrogen temperatures), provides some protection from the electron beam. Whilst negative staining produces a slight distortion of the sample, cryo-prepared samples retain their original shape.

Behaving as a wave, electrons follow the same principles as x-rays (see section 1.10.2), although electrons interact more readily with atoms than do X-rays making it possible for electron diffraction to be observed from a single layer protein crystal (i.e. a 2D crystal, see section 1.9.3). Furthermore, since an image is observed, electron microscopy is a unique technique capable of obtaining both diffraction and phase information. Although it is possible to determine structure from electron microscopy alone, resolutions are generally not above 5Å owing to the thin sample and a low signal to noise ratio due to internal scattering of electrons within the crystal. Radiation damage is another problem associated with electron diffraction. Ideally, samples are prepared using cryo-fixation and a "low dose set-up" used to record diffraction or images. A low dose set up is one in which samples are searched for crystals using a low intensity electron beam, focusing of the sample is done on an area away from the crystal, then finally the crystal is exposed to a higher intensity electron beam. In order to obtain a data, set the sample grid is tilted with respect to the electron beam. The tilting of the sample is a limitation of electron crystallography since the sample can not be completely rotated (90° tilt would put the sample parallel to the electron beam) this means that a "cone" of data will be missing and so a complete data set of a single layer crystal cannot be obtained using current electron diffraction techniques. However, various softwares are available to allow the missing data to be estimated.

1.10.6.   2D Electron Crystallography of Membrane Proteins

A single mammalian 7TMR structure has been solved using 2D crystallisation and electron diffraction, not surprisingly it is that of bovine rhodopsin (Krebs, et al., 1998). A 3.5Å diffraction pattern gave a final structure of 5Å resolution and the structure compared well with that obtained from x-ray crystallography. The protein was partially solubilised from bovine eyes (rod outer segments) using lauryldimethylamine oxide (LDAO). Detergent was removed by dialysis at which time residual bovine membranes provided the necessary

lipidic environment for the receptor. Interestingly, the protein suspension was then separated on a sucrose gradient and crystals only formed in the fraction corresponding to a density of 1.166g/mL.

1.11. Aims and Summary of this Thesis

This PhD thesis reports work towards the atomic resolution structure of a mammalian seven transmembrane receptor (7TMR). Thus the aims of this study are divided into the first three requirements for protein structure and are as follows;

1) Expression of a 7TMR in functional form.
2) Purification of a 7TMR to homogeneity, preferably in functional form.
3) Crystallisation of the receptor using *in meso* (three dimensional) and two-dimensional crystallisation.

The first aim was attempted using recombinant baculovirus infection of insect cells and so required the use of molecular biology techniques to clone and modify receptor genes and construct recombinant baculoviruses. 7TMR expression in the infected *Sf*9 cells was confirmed using radioligand binding. An increase in radioligand binding sites in the hours post infection (in addition to DNA sequencing) demonstrated correct construction of the baculovirus and subsequent expression of the receptor. Expression of the polyHistidine tagged M_2 muscarinic (M_2R) and H_1 histamine receptors (H_1R) was optimised using receptor specific ligand addition to infected insect cell cultures.

Successful production of polyHistidine tagged M_2R and H_1R allowed two areas to be pursued – a) functional reconstitution of the receptors with purified G-proteins and b) purification of the receptors. The first aspect provided initial functional characterisation of the receptors. It also provided the opportunity for initial protein purification experiments. 7M urea treatment semipurified the 7TMR whilst retaining the protein in the membrane. The membrane associated G-proteins were extracted using detergent and purified using immobilised metal affinity chromatography (IMAC). PolyHistidine tagged receptors were also purified by IMAC, with an additional gel filtration chromatography preparing the receptor for crystallisation. Whilst, clearly, it is preferable to prepare a purified receptor that is functional, given the highly challenging target and a desire to develop techniques for *in meso* crystallisation, a purification protocol which produced a mixed population of

functional and non-functional receptor was deemed to be a realistic outcome of this aim of the project. Whilst structure of a non-functional protein would have little physiological relevance it may be useful in future development of purification protocols. Furthermore, use of the partially active receptor allowed development of the techniques required for *in meso* crystallisation, whilst work on the purification protocol was ongoing.

Both two and three dimensional crystallisation of the polyHistidine tagged H_1R was attempted. Three dimensional crystallisation trials were carried out in the mesophase and crystals were analysed by X-ray diffraction. For two dimensional crystals the polyHistidine tagged H_1R was reconstituted into lipids and the detergent removed. Two dimensional crystals were formed in suspension and analysed by electron microscopy and electron diffraction.

2. Expression of Seven Transmembrane Receptors in *Spodoptera frugiperda* Cells

2.1. Acknowledgements

2.2. Introduction

Insect cell culture has proven valuable for recombinant protein expression due to a combination of its low maintenance requirements and ability to perform post-translational protein modification (Massotte, 2003). The *Spodoptera frugiperda* (*Sf*)21 cell line was originally prepared from the ovaries of the 'fall armyworm', moth (Vaughn, et al., 1977). The clonal *Sf*9 cell line was derived from the *Sf*21 parent. *Sf* cells are a target for the *Autographa californica* multiple polyhedrosis virus (AcMPV), so named for the characteristic crystal like protective polyhedra protein coat that is formed about the infective particle. Foreign protein expression in *Sf* cell lines can be achieved by production of recombinant baculoviruses. The production of recombinant baculovirus was significantly improved in 1997 by the production of an *E.coli* cell line which contained modified baculovirus DNA (Ciccarone, et al., 1997). Tn7 attenuation sites were incorporated into the baculovirus DNA which, along with a Tn7 transposase helper plasmid, is maintained in DH10Bac *E.coli*. Attenuation sites in the baculovirus DNA (also referred to as "bacmid") compliment the shortened Tn7 transposition sites incorporated into a donor plasmid. After cloning of the gene of interest into the donor plasmid, DH10Bac provides the necessary components for site specific recombinant of the gene (and flanking regions) from the donor plasmid into the baculovirus DNA. Prior to the development of the DH10Bac method of recombination, baculovirus production was a more time consuming process in which recombinantion of baculovirus DNA and the donor vector occurred in the insect cell and successful recombination was detected by plaque assay. The flanking region of the donor plasmid includes the promoter which will ultimately control transcription of the gene with this promoter commonly being the polyhedrin promoter of AcMPV. The polyhedrin promoter is a late promoter in the virus lifecycle, resulting in maximum gene transcription at approximately 50-60 hours post infection (hpi). Recombinant baculovirus DNA purified from the DH10Bac is used to transfect *Sf* cells using lipid mediated delivery. Once in the cell, the recombinant viral DNA can replicate and be packaged as mature virus particles by the host cell. Baculovirus infected cells begin to lyse at approximately 72 hpi, at which time viral particles are collected from the cellular supernatant. Viral particles can then be further amplified or used to infect subsequent insect cell cultures. On recombinant virus addition to insect cells, the virus inserts its DNA into the insect cell (infection) and migrates to the nucleus where expression of the desired gene occurs through the polyhedrin promoter.

Many members of the 7TMR family have been expressed using the baculovirus/Sf cell system, often in higher yields than that obtained in mammalian cell lines (Massotte, 2003). Several publications have reported the expression of the M$_2$R in Sf9 cells. Rinken, et al., (1994) reported an expression level of 4pmol/mg (determined by [^{3}H]-scopolamine binding) for human M$_2$R expressed in baculovirus infected Sf9 cells. Receptor type was confirmed by the nM affinity of [^{3}H]-scopolamine to sites on the Sf9 membranes and by a rank order potency of atropine > pirenzepine >>carbachol to these same sites (Rinken, et al., 1994). Weill, et al., (1997) reported a similar expression level for the human M$_2$R in baculovirus infected Sf9 cells. Interestingly, Weill, et al., (1997) observed a maximum expression of 3pmol/mg at six days after infection. Parker, et al., (1991) reported a considerably higher expression of 30pmol/mg total cellular protein for the human M$_2$R. Different radioligands were used to detect the M$_2$R which may explain the difference in measured expression level, although both ligands have low nM affinity for the receptor. Parker, et al., (1991) used [^{3}H]-QNB saturation binding for determination of M$_2$R expression level, whilst both Rinken, et al., (1994) and Weill, et al., (1997) used [^{3}H]-scopolamine. Ratnala, et al., (2004) reported 40 – 50pmol/mg expression of a human H$_1$R using baculovirus/Sf9 cells which was significantly higher than the 3 – 5 pmol/mg expression reported by Houston, et al., (2002) using the same receptor and expression system. The same H$_1$R baculovirus used by Ratnala, et al., (2004) was used in this study (see section 2.3.2).

Receptor association with the outer cell membrane is a dynamic process with receptors being recycled between the outer cell membrane and inner cell compartments (Xu, et al., 2007). The movement of the receptor is modulated by the extracellular ligand environment; typically, prolonged exposure of a receptor to an agonist results in receptor internalisation and prolonged exposure to inverse agonist/antagonist in an increase in receptor on the cell surface (May, et al., 2005; Milligan and Bond, 1997; Xu, et al., 2007). Internalisation is associated with desensitization of the receptor, a phenomenon defined as reduction of 7TMR/G-protein signaling (Pierce, et al., 2002). Clinically, receptor trafficking has importance in terms of drug dependence and tolerance. For recombinant protein over-expression, the ability to modulate membrane associated receptor number may present a simple method for optimising receptor over-expression.

Receptor ligand binding assays utilize the specific interaction of a receptor with its cognate ligands and thus can provide a useful initial assessment of recombinant protein expression. This is particularly the case for 7TMRs which, due to their low expression, membrane association and a lack of appropriate primary antibodies, can be difficult to detect using the Western blot technique. Saturation ligand binding assays determine the number of ligand binding sites (receptor) in a given sample. The labeled ligand concentration is increased to an amount which causes all receptors in the sample to be occupied by ligand. In this study, all such ligands were labeled with the β decaying tritium ($[^{3}H]$). Non-specific binding of the labeled ligand is determined by simultaneous addition of an unlabelled ligand for the receptor. Competition binding assays, which use log concentrations of unlabelled ligand in addition to the labeled-ligand, provide further characterisation of the labeled-ligand binding site (receptor).

The aim of this study was to produce a selection of 7TMRs using the baculovirus/*Sf*9 expression system. An additional aim was to express these receptors such that they would be amenable to purification at a later date and this meant addition of an affinity tag to the receptor as well as some optimisation of the receptor expression. Three receptors were chosen for study, the M_2 muscarinic, H_1 histamine and $5HT_{2A}$ serotonin receptors. This allowed progressive selection of the most suitable receptor for expression, purification and potentially crystallisation.

2.3.   Materials and Methods

2.3.1. General Materials

Unless otherwise stated in the text, all chemicals and reagents were of analytical grade and were purchased from Sigma Aldrich. All buffers were made in milli-Q treated water (mQH_2O).

2.3.2. Construction of Baculoviruses

The following four sections describe the general procedures for cloning, producing recombinant baculovirus DNA and for producing the mature virus. This is proceeded by methods which are specific for each receptor.

Cloning of receptor DNA into pFastBac1 (general)

Receptor cDNA was amplified by the polymerase chain reaction (PCR) with primers containing receptor coding sequence, appropriate restriction enzyme recognition sequences and modifying sequences (such as hexa- or deca- Histidine tagging). Forward and reverse primers (0.5µg of each) were combined with equimolar dNTPs (6.25nmol), $MgCl_2$ (5nmol), 10X NH_4 Reaction Buffer (2.5µL, Bioline), BIOTAQ^{TM} Polymerase (5 units/µL, Bioline) and between 0.5 and 2µL of template, depending on the template source, with a final PCR reaction volume of 25µL. Template DNA was initially denatured at 95^oC for 3 minutes. The template was amplified using between 25 and 35 cycles of: DNA denaturation (95^oC, 30 seconds), primer annealing (56^oC, 90 seconds) and polymerase extension (72^oC, 90seconds). A single extension at 72^oC for 5 minutes, completed the amplification process. PCR products were loaded on a gel consisting of 1% (w/v) agarose in TAE (0.04M Trizma$^®$ Base, 0.02M Acetic acid, 1.27mM EDTA) buffer and electrophoresis carried out at 120V. DNA was visualised by staining of the gel in a bath of ethidium bromide/TAE and exposure to UV light. PCRs producing a single product (or when mixed products were less than 300bp) were removed from reaction components using the PureLink^{TM} Purification kit (Invitrogen) following manufacturer's instructions. Where the PCR produced more than one product, the entire reaction was separated by agarose gel electrophoresis and the desired DNA product excised from the gel. DNA was extracted from the agarose matrix using QIAquick Gel Extraction Kit (Qiagen) following manufacturer's protocol. Purified PCR product, or pFastBac1 (Figure 1, Invitrogen), was

digested with appropriate restriction enzymes (New England Biolabs) according to manufacturer's instructions.
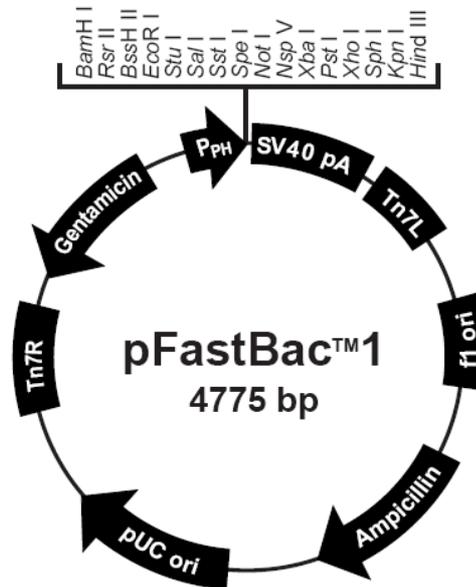
Figure 1. Map for pFastBac1 (Invitrogen). For construction of the C terminal His-tagged M_2R constructs, receptor DNA was cloned into the *Kpn*I/*Hin*dIII site. All sequence between the transposition sites (Tn7R and Tn7L) is transferred to the baculovirus DNA contained in DH10Bac. The polyhedrin promoter (P_{PH}) drives expression of the gene once recombinant baculovirus has been produced.

Reactions were carried out at the enzyme's optimal temperature (37^oC for *Kpn*I and *Hin*dIII) for between 4 and 24 hours. DNA was purified from restriction digest components using the PureLink^{TM} purification kit. Amplified and digested receptor cDNA was combined with digested pFastBac1 (50ng) in a 1:3 Molar ratio of vector:insert in sterile mQH$_2$O to a final volume of 10μL. Quick Ligase Buffer (10μL of a 2x stock, New England Biolabs) was added to the plasmid/insert mixture, followed by addition of Quick T4 DNA ligase (1μL, New England Biolabs). The ligation reaction was carried out at room temperature for 5 minutes and terminated by placing on ice. The ligation reaction was immediately transformed into chemically competent DH5α. Ligation mixture (5ng) was added to *E.coli* (50μL), gently mixed and incubated on ice for 20 minutes. Cells were then "shocked" at 37^oC for 2 minutes, followed by replacement on ice for 5 minutes. Between 200 and 500μL of room temperature Luria Bertani media (LB, 1% w/v Tryptone, 0.5% w/v Yeast Extract, 1.0% w/v NaCl, pH 7.0) was added to the cells which were then cultured at 37^oC for 5 hours, before being plated on LB agar (LB media containing 1.5% w/v agar) containing 100μg/mL Ampicillin. Plates were placed at 37^oC overnight or until bacterial colonies were of sufficient size to be easily visible. Antibiotic selected colonies were

screened for correct insert by carrying out PCR using the bacteria as a template, or by restriction digest of plasmid DNA which had been extracted from an overnight culture of the bacterial colony. The plasmid DNA was extracted using GenElute Plasmid Miniprep kit (Sigma Aldrich), following manufacturer's instructions. PCR was carried out using a combination of gene specific and vector specific primers. Correct construction of the recombinant vector was confirmed by DNA sequencing (IMVS sequencing facility, South Australia).

Construction of recombinant baculovirus DNA (general)

The confirmed recombinant pFastBac construct (1ng) was gently combined with competent DH10Bac^{TM} (100μL, Invitrogen), uptake of the vector was promoted by the heat shock method described above, cells were grown in SOC media (2% w/v tryptone, 0.5% w/v yeast extract, 10mM NaCl, 2.5mM KCl, 10mM MgCl$_2$, 10mM MgSO$_4$, 20mM glucose). After 5 hours of growth, cells were plated onto LB Agar plates containing Kanamycin (50μg/mL), Gentamycin (7μg/mL) and Tetracycline (10μg/mL) for DH10Bac selection, and IPTG (40μg/mL) and X-gal (100μg/mL) for detecting *LacZ* interruption. Plates were placed at 37°C overnight or until colonies were readily visible. White DH10Bac colonies were isolated and added to LB (~4mL) containing Kanamycin, Gentamycin and Tetracycline (concentrations as above) prior to overnight growth at 37°C. Baculovirus DNA (bacmid) was extracted from the overnight DH10Bac culture using a procedure modified from the manufacturer's instructions. Briefly, DH10Bac cells (1.5mL) were collected by centrifugation (14000rpm, 1 minute) and re-suspended in 300μL solution I (15mM Tris-HCl pH8.0, 10mM EDTA, 100μg/mL RNase, filter sterilized, stored at 4°C). 300μL of solution II (0.2N NaOH, 1% SDS, filter sterilized, stored at RT) was added and the lysate incubated at room temperature for 5 minutes. Cellular protein and genomic DNA was precipitated by addition of 300μL of solution III (3M Potassium Acetate, pH 5.5, autoclaved, stored at 4°C). The reaction was placed on ice for 20 minutes before separation of the precipitate by centrifugation (14000rpm, 30 minutes, 4°C). The bacmid containing supernatant was added to 800μL of isopropanol and the reaction either placed on ice for 3 hours or at -20°C overnight. The isopropanol bacmid DNA extract was collected by centrifugation (14000rpm, 30 minutes, 4°C) and gently washed with 70% (v/v) ethanol. The DNA was briefly placed at room temperature to facilitate near drying of the pellet, before re-suspension in sterile mQH$_2$O (smQH$_2$O). Bacmid was analysed for correct construction using the PCR with a combination of gene and bacmid specific primers.

Bacmid specific primers were designed as follows M13(40)_F (5′d[GTT TTC CCA GTC ACG AC]3′), which annealed 5' to the bacmid transposition site and M13_R (5′d[CAG GAA ACA GCT ATG AC]3′) which annealed 3' to the transposition site.

Transfection of *Sf*9 cells with recombinant bacmid and production of baculovirus (general)

Correctly constructed bacmid (1μg) was made up to 194μL with un-supplemented Grace's Medium (Invitrogen) and 6μL of Cellfectin (Invitrogen) was added. DNA/lipid complex formation was promoted by room temperature incubation for 30 minutes. On completion of the incubation the mixture was made up to 1mL with Sf900-II serum free insect culture media (Invitrogen). Approximately 1×10^6 *Sf*9 cells were pelleted (750xg, 3 minutes) and gently re-suspended using the filter (0.2μm) sterilized DNA/lipid media. To allow uptake of the bacmid into the cells, suspended cells were incubated at 27^oC with orbital shaking (140rpm on Raytek Orbital Mixer Incubator) for 4 hours. Cells were collected (750xg, 3 minutes), the DNA/lipid media removed and the cells re-suspended in Sf900-II media containing Penicillin (50 units/mL) and Streptomycin (50μg/mL). Cultures were analysed for signs of bacmid infection by light microscopy and staining with Trypan Blue (0.05% in PBS, diluted 1:1 with cells) 72 hours post DNA transfection. Cells were subsequently monitored every 24 hours within which cell morphology changes and a decrease in cell viability generally became noticeable 120 hours (5 days) post transfection. At this time cells were pelleted (750xg, 10 minutes) and the supernatant collected and filter (0.2μm) sterilized. This supernatant represented the P1 viral stock, P2 stock was generated in a 10mL *Sf*9 culture by addition of 1mL of the P1 virus. P2 virus was collected 72 hours post infection, at which time signs of viral infection were visible. P3 stock was generated by addition of 5mL of virus to 100mL of culture. P3 viruses were assumed to have infectivity of 5×10^7p.f.u/mL. This was confirmed by plaque assay for the N terminal His tagged M_2 muscarinic receptor. Cells pelleted from P3 baculovirus production were collected and intracellular baculovirus DNA extracted using the method described above. This DNA was used as a template for PCRs using a combination of bacmid and gene specific primers, to confirm the presence of the baculovirus DNA and the gene of interest. Collected virus containing supernatants were filter sterilised with 2-3% fetal bovine serum (v/v, final concentration) and stored, in the dark, at 4^oC.

Amplification of baculoviruses (general)

Following production of the P3 viral stock, virus stocks were maintained by infection of *Sf*9 cells using an MOI of 0.1. The amount (mL) of virus to add was determined using equation 1.

$$\text{Virus required (mL)} = \frac{\text{desired MOI x total no. cells}}{\text{viral titre (PFU)}}$$

Equation 1. Calculation of virus (mL) addition for amplification of virus. MOI = 0.1 and plaque forming units (PFU) = 5×10^7 pfu/mL

72 hours post infection cells were pelleted (750xg, 15 minutes) and the virus containing supernatant collected and filter sterilised with FBS as described above. The cells were discarded.

Specific M_2 Muscarinic Receptor Construct Methods

Baculovirus encoding the human form of the M_2 Muscarinic Receptor was a gift, arranged by Dr Wayne Leifert (Commonwealth Scientific and Industrial Research Organisation – CSIRO), from the laboratory of Professor Alfred Gilman, University of Texas Southwestern Medical School, Dallas, Texas. M_2 Receptor coding sequence DNA was obtained by extracting bacmid from M_2R baculovirus infected *Sf*9 insect cells and using it as a template in a PCR with M_2R targeting primers. The N terminal hexa-Histidine tagged M_2 receptor baculovirus was produced by Dr Richard Glatz (South Australian Research and Development Institute (SARDI), formerly CSIRO). The M_2R sequence was cloned into pFastBacHT (Figure 2, Invitrogen) using the same methods for insertion of receptors into pFastBac1. M_2R/pFastBacHT was then transformed into DH10Bac and the general methods described above were used to prepare the mature recombinant virus.
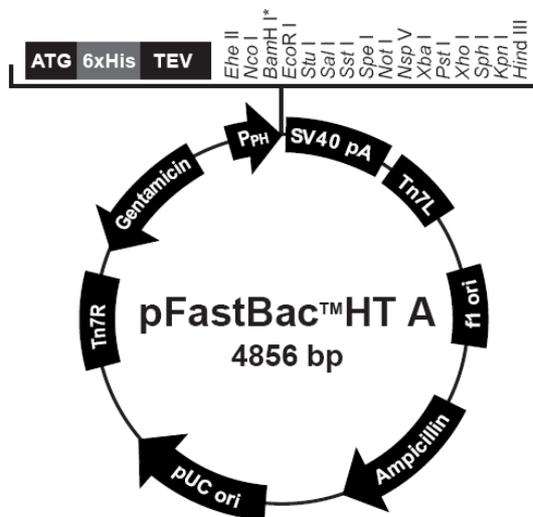
Figure 2. Map of pFastBacHT-A (Invitrogen). Cloning of the M_2R coding sequence into this vector was used to produce the $His6_NM_2R$ baculovirus. The M_2R/pFastBacHT-A is transformed into DH10Bac and recombinantion with the baculovirus DNA occurs at the transposition sites Tn7R and Tn7L.

C terminal hexa-Histidine ($His6_C$) tagged receptor DNA was obtained by PCR with the primer *Kpn*I_M_2R_F (5'd[GCGC GGC ACC ATG AAT AAC TCA ACA AAC TCC]3') and the primer *Hin*dIII_M_2R_R (5'd[CG AAG CTT TTA GTG ATG GTG ATG GTG ATG CCT TGT AGC GCC TAT GTT]3') containing sequence for hexa-Histidine addition prior to the stop codon. For the deca-Histidine construct an additional 18 nucleotides (ATG/GTG) were incorporated. The product from this PCR was digested with *Kpn*I and *Hin*dIII and ligated into pFastBac1, as described above. Correct vector construction was confirmed using the primers pFB1_F (5'd[GGA TTA TTC ATA CCG TCC]3') and pFB1_R (5'd[CTA CAA ATG TGG TAT GGC]3') which bound to the vector polyhedrin promoter and SV40 polyadenylation signal, respectively.

Specific $5HT_{2A}$ Serotonin Receptor Construct Methods

cDNA for the human form of the $5HT_{2A}$ receptor was obtained in pDEST8 (Figure 3, Invitrogen) and purchased from imaGenes (formerly RZPD, the German Resource Centre for Genome Research, http://www.imagenes-bio.de/). Sequence was confirmed by the supplier and by the purchaser using primers pDEST_F (5'd[AGT TTG TAC AAA AAA GCA GGC]3') and pDEST_R (5'd[GTG AAA CAT GTT CTA AGC TGG GT]3') which bound to the vector attenuation sites B1 and B2 respectively. The vector was transformed into DH10Bac and baculovirus produced as described above. The $His6_C5HT_{2A}R$ baculovirus was produced by Dr Janelle Williams (CSIRO MHT).
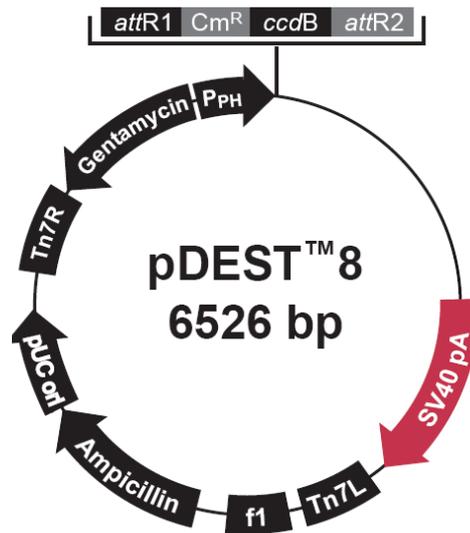
Figure 3. Map of pDEST8 (Invitrogen). 5HT$_{2A}$R coding sequence was purchased in this vector. Transposon sites (Tn7R and Tn7L) allow for recombinantion with recombinant baculovirus DNA within DH10Bac. pDEST8 is a Gateway^{TM} vector.

Specific D$_{2L}$ Dopamine Receptor Construct Methods

cDNA for the human form of the D$_2$ receptor was obtained in pDEST8 (Invitrogen) and purchased from imaGenes. D$_2$R recombinant baculovirus was produced by Dr Janelle Williams (CSIRO).

Specific H$_1$ Histamine Receptor Baculovirus Information

No cloning steps were performed on the H$_1$R. Baculovirus encoding a C terminal deca-Histidine tagged form of the human H$_1$ Histamine receptor was generously supplied by Professor Wim deGrip of the Nijmegen Centre for Molecular Life Sciences (NCMLS) through a material transfer agreement with Professor Ted McMurchie of the Commonwealth Scientific and Industrial Research Organisation (CSIRO).

2.3.3. Cell Culture and Baculovirus Infection for Receptor Expression

*Sf*9 cell growth and baculovirus infection (general)

Suspension cultures of *Sf*9 insect cells were grown, using Sf900-II media (Invitrogen), in sterilized Schott bottles with a loosened lid to allow airflow. Culture volumes were generally no more than ¼ of the total bottle volume. To maintain approximate *Sf*9 cell densities of between 0.7×10^6cells/mL and 3×10^6cells/mL, cells were diluted on the first, third and fifth day of each week. For baculovirus infection, cells were grown to an approximate density of 2×10^6cells/mL and freshly filter-sterilized baculovirus added at an

approximate multiplicity of infection (MOI) of 2, using equation 1. P3 baculovirus, and subsequent amplifications of the viral stock, were used for protein production. Unless otherwise stated, cell viability was assessed at 72 hours post infection and cells harvested (1500xg, 15 minutes) for immediate membrane preparation or frozen in liquid Nitrogen for future use.

Expression Time Course Studies

After infection with recombinant baculovirus, insect cells were collected (1000×g, 10 min) at 24 hour intervals and resuspended in 'incubation buffer' (250 mM Sucrose, 10 mM Tris pH 8.0, 3 mM $MgCl_2$, Phenylmethyl Sulfonyl Fluoride (PMSF, 0.02mg/mL), Benzamidine (0.03mg/mL), Bacitracin (0.025mg/mL) and Soya Bean Trypsin Inhibitor (0.03mg/mL). Cells were frozen in liquid nitrogen and stored at -80°C.

Expression of 7TMRs in the presence of receptor specific ligands (ligand culture)

To determine the effect of addition of receptor ligand to infected cultures, cells were infected with recombinant baculovirus as described above. To limit variability in cells prior to ligand addition, cells were infected in a single bottle and were separated immediately preceding addition of the ligand. For $M_2R/D_{2L}R$, 24 hours prior to harvest (48 hours post infection) the ligand was mixed with 1-3mL (no more than 1% of total culture volume) of media and filter sterilized into the infected cell culture using a 0.2μm filter (Millipore). Ligands were used at the concentrations shown in Table 1.

Table 1. Final concentration of ligands used in baculovirus infected *Sf*9 culture. NPA = norapomorphine

Receptor:

M_2 Muscarinic	H_1 Histamine	D_{2L} Dopamine
Atropine 50nM	Triprolidine 20nM	Haloperidol 50nM
Pirenzepine 50nM	pyrilamine 150nM	Bromocryptine 10μM
Acetylcholine 20μM	Histamine 20μM	NPA 10μM

Cells were collected at 72 hours post infection and membranes were prepared as described below. For the H_1R, ligand was added at 72 hours post infection and cells collected at 96 hours post infection.

2.3.4. Receptor Membrane Preparation

All steps were carried out on ice or at 4°C unless otherwise stated.

Infected *Sf*9 cells (1L) were collected and centrifuged at 1000×g for 10 min and re-suspended in 125 ml ice-cold 'lysis buffer' (50 mM HEPES pH 8.0, 0.1 mM EDTA, 3 mM MgCl$_2$, 10 mM β-Mercaptoethanol) with protease inhibitors; 0.02 mg/mL PMSF, 0.03 mg/mL Benzamidine, 0.025 mg/mL Bacitracin and 0.03 mg/ml Soy Bean Trypsin Inhibitor. Cells were subjected to N$_2$ cavitation at 500 psi (3400 kPa) for 15 min, followed by sedimentation of nuclei and unbroken cells (750×g, 10 min). Membranes were pelleted by centrifugation of the supernatant at 100,000×g for 30 min. Endogenous G-proteins were removed from *Sf*9 membranes by modification of a published method (Lim and Neubig, 2001). The 100,000×g membrane pellet was resuspended (50 mL) in 'incubation buffer' (as above) containing 7 M urea. After 30 min stirring the membranes were diluted to 4 M urea with 'incubation buffer' and protease inhibitors and centrifuged at 100,000×g for 30 min. The urea-treated membrane pellet was washed twice in 'incubation buffer'. The final urea-treated membrane pellet was resuspended to approximately 1–3 mg/ml protein and aliquots were rapidly frozen in liquid N$_2$ and stored at −80°C until use. Protein concentration was determined by the Bradford protein assay (Bradford, 1976).

2.3.5. Ligand Binding Assays

<u>Saturation Binding Assays</u>

Membrane protein and appropriate radioligand were diluted in TMN buffer (50mM Trizma$^®$, 10mM MgCl$_2$, 100mM NaCl, pH7.6), typically to a final volume of either 75 or 100μL. [^{3}H] labelled forms of scopolamine, pyrilamine and ketanserin (Perkin Elmer) where used for the M$_2$, H$_1$ and 5HT$_{2A}$ receptors respectively. Final membrane protein concentration in the assay was determined such that less than 10% of total radioligand was receptor bound. Non-specific radioligand binding was determined by addition of unlabelled ligand to the reaction mix; atropine (10μM) for the M$_2$R, triprolidine (10μM) for the H$_1$R and ketanserin or clozapine (15μM or 10μM) for the 5HT$_{2A}$R. Assays were incubated, with shaking, in a 27°C water bath for 60 minutes. The reaction was terminated by rapid filtration over glass microfibre filters (Adelab). Filters were washed with 3 x 3mL of ice cold TMN buffer. Filters were placed in Pico Pro Vials™ (Perkin Elmer) and covered in 3mL of Ultima Gold™ (Perkin Elmer) liquid scintillant. Beta radiation was detected in a Wallac 1410 Liquid Scintillation Counter (Pharmacia, Perkin Elmer).

<u>Competition Binding Assays</u>

Assays were prepared as described above. [^{3}H]-ligand concentration was fixed at the approximate K_d value for the radioligand/receptor interaction. Log dilutions of competing unlabelled ligand were prepared in TMN buffer and added to the assay (instead of addition of the fixed concentration of unlabelled ligand).

2.3.6. Data Analysis

Graphs were produced using Prism4 (GraphPad Software). Saturation binding curves were best fitted to one-site binding models with non-linear regression.

2.4. Results and Discussion

2.4.1. Cloning and production of baculoviruses

M$_2$R baculoviruses

In this study His-tagged proteins were prepared in preparation for immobilised metal affinity chromatography (IMAC). The length of the Histidine tag was varied in order to produce a receptor construct which showed a combination of optimal expression and optimal binding to the IMAC resin. Previous studies have demonstrated an increase in the affinity of Nickel binding by Histidine tags of increasing length (Barton, et al., 2007). Optimal placement of the Histidine tag varies between protein, therefore three M$_2$R baculoviruses were constructed for this study as defined in Figure 4. The His6$_N$M$_2$R baculovirus was constructed by Dr Richard Glatz (SARDI) and contained a Tobacco Etch Virus (TEV) protease site 3' to the 6x His tag. Whilst the TEV site would facilitate removal of the Histidine tag should it become necessary at a later date, at this stage of the project it was not considered to be essential that the Histidine tag be removed. Thus, a protease site was not incorporated in the C terminal Histidine tagged M$_2$R constructs. Furthermore, addition of a TEV site would have left six additional amino acids on the receptor C terminus following protease cleavage at the site, essentially negating any advantage of removing the Histidine tag.
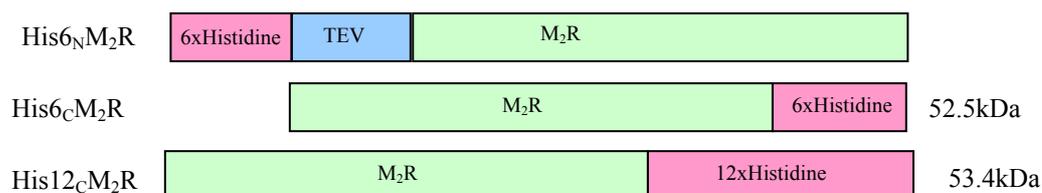

Figure 4. M$_2$R constructs produced in baculovirus for *Sf*9 cells. TEV = tobacco etch virus protease site.

A PCR using the primers *Kpn*I_M$_2$R_F and *Hin*dIII_M$_2$R_F (which contained coding sequence for His6$_C$) gave a PCR product of between 1000 and 1500 base pairs (bp) (Figure 5A), as was expected for the 1398bp His6$_C$M$_2$R sequence. Following cloning of the gene into pFastBac1 and transformation of the His6$_C$M$_2$R/pFastBac1 recombinant plasmid into DH5α, putative recombinant plasmid containing colonies were isolated, grown and the plasmid extracted. Restriction digest of the extracted plasmid with *Kpn*I and *Hin*dIII

removed the His6$_C$M$_2$R DNA fragment from the plasmid as indicated by the presence of ~1400bp fragment when the restriction digest was separated by agarose-gel electrophoresis (Figure 5B). At this time the plasmid was sequenced and the His6$_C$M$_2$R coding sequence was confirmed.
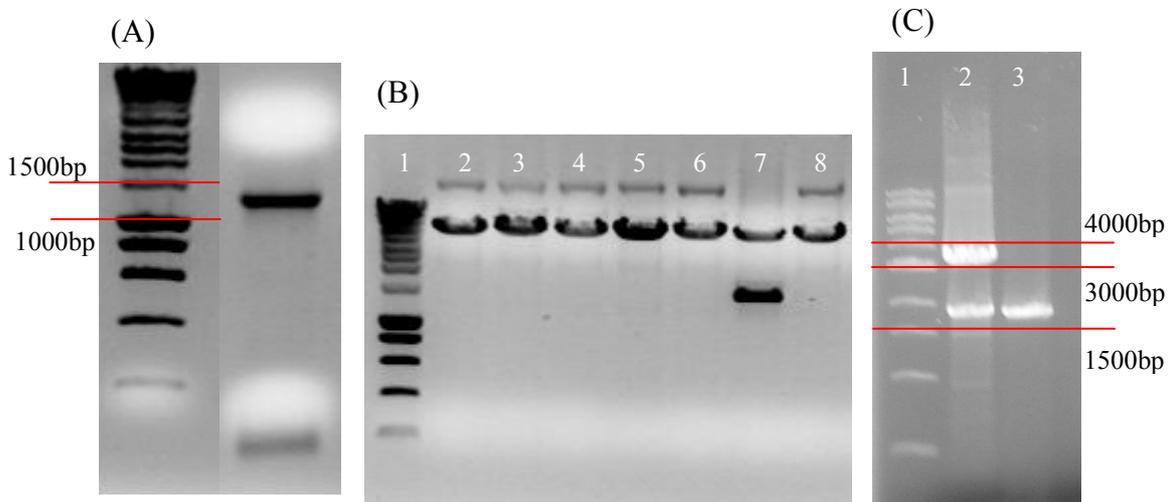

Figure 5. (A) PCR of M$_2$R bacmid with *Kpn*I_M$_2$R_F and HindIII_M$_2$R_h6_R. (B) KpnI/*Hin*dIII restriction digest of putative pFB1_M$_2$R_h6. Lane Descriptions: 1-6 and 8 – Non-recombinant pFB1; 7 – digested pFB1_M$_2$R_h6. (C) PCR of isolated M$_2$_h6 bacmid with; lane 2 – bacmid specific primers, lane 3 – *Kpn*I_M$_2$R_F and bacmid reverse.

After infection of *Sf*9 cells with the P3 His6$_C$M$_2$R baculovirus (see section 2.3.3), insect cells were collected and the baculovirus DNA extracted. PCR using M13 primers on bacmid containing a 1400bp insert should produce a 3800bp fragment, as was observed (Figure 5C, lane 2), M$_2$R specific primers then confirmed the 1400bp fragment to be the receptor DNA (Figure 5C, lane 3). Thus, this final PCR analysis demonstrates the presence of the His6$_C$M$_2$R gene, correct incorporation of the gene into the baculovirus DNA and the ability of the virus to infect and be replicated in *Sf*9 cells. These analyses were performed on all viruses produced in this study.

5HT$_{2A}$R baculovirus

cDNA for the 5HT$_{2A}$R was obtained in pDEST8 (Figure 3, Invitrogen). The transposition sites in pDEST8 allow for direct transformation of the recombinant vector into DH10Bac. Since expression of this receptor using the baculovirus/insect cell system had not been previously reported, a baculovirus encoding the un-tagged form of the receptor was constructed first to allow initial assessment of receptor expression prior to performing lengthy cloning procedures. As was done for the muscarinic receptor baculoviruses,

assessment of the recombinant $5HT_{2A}R$ baculovirus was achieved by performing the PCR on baculovirus DNA isolated from P3 *Sf*9 cells (Figure 6). A combination of gene (Figure 6, lane 2) and bacmid (Figure 6, lane 4) specific primers confirmed the presence of the 1413bp $5HT_{2A}R$ gene in the bacmid and infectivity of the baculovirus.
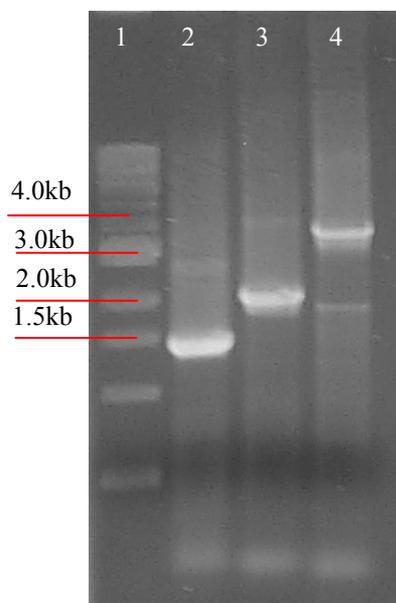

Figure 6. PCR analysis of putative $5HT_{2A}R$ bacmid. Lane Descriptions; 2 – PCR of bacmid with $5HT_{2A}R\_F$ and $5HT_{2A}R\_R$; 3 – PCR with $5HT_{2A}R\_F$ and M13_R; 4 – PCR with M13_F and M13_R.

P3 virus stock (refer to section 2.2.2) was used for subsequent infection of *Sf*9 cells for protein production.

2.4.2. Expression of the M_2 Muscarinic Receptors

Further confirmation of correctly constructed baculovirus and preliminary optimisation of receptor expression was achieved by measurement of receptor binding sites following viral infection of the cells. A gene under the control of the baculovirus polyhedrin promoter will undergo maximum transcription at between 40 and 50 hours post infection, thus maximum protein expression is expected 15 – 20 hours after this. *Sf*9 cells infected with the $His6_CM_2R$ baculovirus demonstrated an increase in saturable $[^3H]$-scopolamine binding sites in the hours following infection (Figure 7)[2].

---

[2] For ease of comparison, B_{max} values have been reported in bar graph format. For complete saturation binding curves, including replicates and K_d values, of all bar graphs presented in this chapter please see chapter 2 appendix.
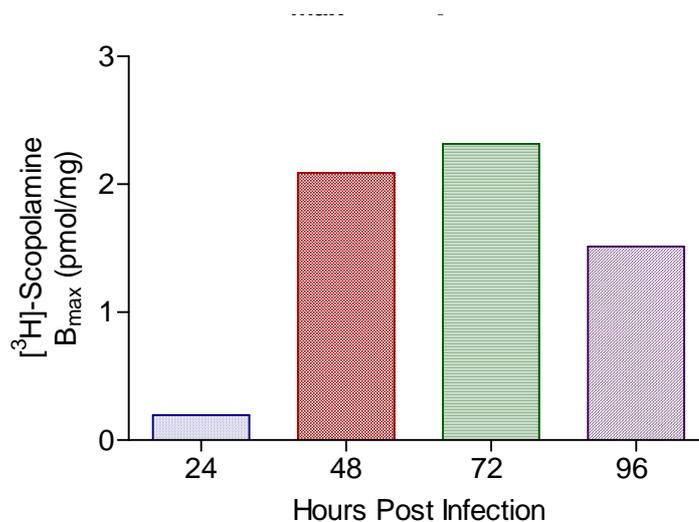
Figure 7. [³H]-scopolamine binding (pmol/mg of total membrane protein) to cells infected with His(6$_c$)M$_2$ recombinant baculovirus. Cells were collected at 24 hour intervals post baculovirus addition and assayed for specific [³H]-scopolamine binding. Non-specific binding was determined in the presence of 10μM atropine. B$_{max}$ values were calculated from saturation curves consisting of data points for which the mean ± S.E.M was calculated for three separate experiments.

In the 96 hours following His6$_C$M$_2$R baculovirus addition, [³H]-scopolamine binding on whole cell lysates increased from near zero, reaching a maximum of ~2.5pmol/mg of total cellular protein at 72 hours post infection. The increase in [³H]-scopolamine binding sites in the hours post infection, along with DNA sequencing and PCR analysis of insect cell extracted bacmid, validates the construction of a His6$_C$M$_2$R recombinant baculovirus and demonstrates the virus ability to infect *Sf*9 cells.

7M urea treated membranes prepared from insect cells infected with wildtype M$_2$R encoding baculovirus showed a single [³H]-scopolamine binding site with nanomolar affinity for the ligand (Figure 8). B$_{max}$ values for the binding site where typically in the range of 15-20pmol per mg of total membrane protein. Previously reported studies have quoted expression levels of between 20-30pmol/mg for M$_2$R expression in baculovirus infected Sf9 cells (Parker, et al., 1991). M$_2$R expression in CHO cells has been reported at 5.5fmol/105 cells (May, et al., 2005).
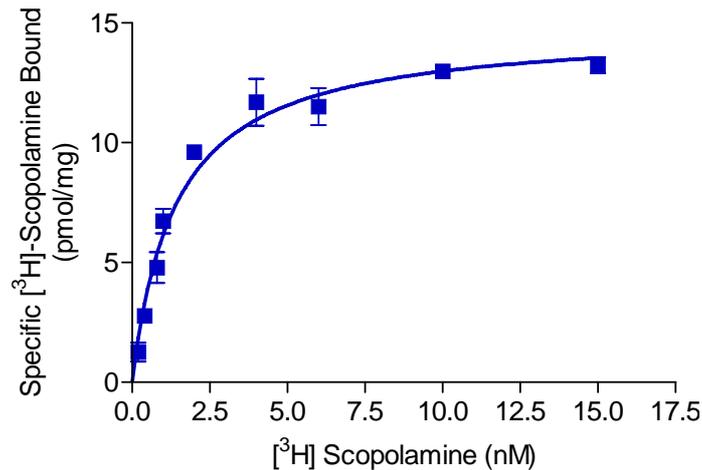
Figure 8. [^{3}H]-Scopolamine binding to membranes prepared from *Sf9* cells infected with M_2R recombinant baculovirus. Non-specific binding was determined in the presence of 10μM atropine. Analysis confirmed a single [^{3}H]-scopolamine binding site which had a 1.4nM dissociation constant for the radioligand. Receptor binding sites were saturated at 14.8 pmol/mg of total membrane protein. Data points represent the mean ± S.E.M, n=3.

Pharmacologically the [^{3}H]-scopolamine binding site matched with the expected profile of the M_2R, showing a rank order potency of atropine > pirenzepine > acetylcholine (Figure 9) (Weill, et al., 1997). The un-tagged M_2R provided the standard from which to measure the effect of tag addition to the receptor.
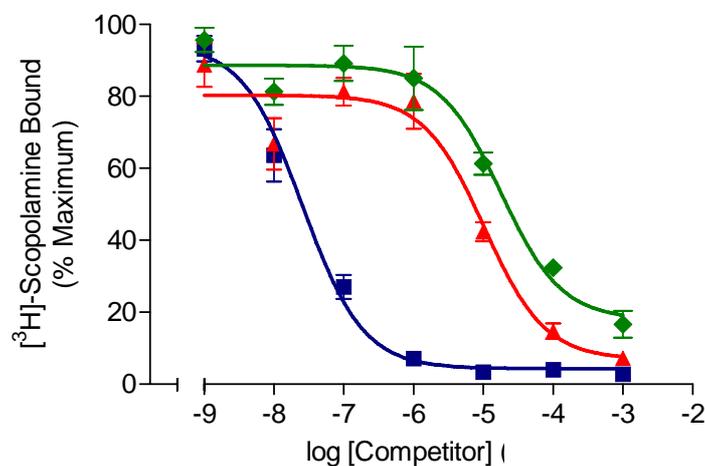
Figure 9. Competition Binding of [^{3}H]-Scopolamine at the M_2R in the presence of the designated concentrations of atropine (blue squares), pirenzepine (red triangles) and acetylcholine (green diamonds). Total protein concentration was 0.05μg/μL, [^{3}H]-Scopolamine concentration was 1nM, filtered assay volume was 100μL. EC_{50} values were calculated based on a one site sigmoidal dose response and were 26.0nM, 10.3μM and 17.0μM for atropine, pirenzepine and acetylcholine respectively. Each data point represents the mean ± S.E.M, n=3.

A hexa-Histidine tag was added to either the N or the C terminus of the muscarinic receptor. Membrane associated expression of the $His6_CM_2R$, as determined by $[^3H]$-scopolamine binding, showed an approximately 33% decrease in expression as compared to the wild type receptor expression (compare Figure 8 and Figure 10B). This is in contrast to Hayashi and Haga, (1996), who reported a $[^3H]$-QNB determined expression level of 36pmol/mg for both a wildtype M_2R and a mutant (N terminal Asparagines replaced with Aspartic Acid) C terminal hexa-Histidine tagged M_2R. There appear to be few reports of N terminal tagged 7TMRs, likely because of an anticipated decrease in membrane associated receptor due to interference of the tag with cellular trafficking of the receptor to the membrane. This may indeed explain the decrease in membrane associated $His6_NM_2R$ compared to M_2R (compare Figure 10A and Figure 8). Alternatively, the perceived difference in membrane associated $His6_NM_2R$ may in fact be a result of a difference in $[^3H]$-scopolamine binding properties of the His tagged M_2R since the N terminal tag may interfere with the receptor orthosteric ligand binding site. Interestingly, there was no significant difference in expression between N terminal or C terminal tagged M_2R, nor hexa- or dodeca- C terminal His tagged M_2R (Figure 10).
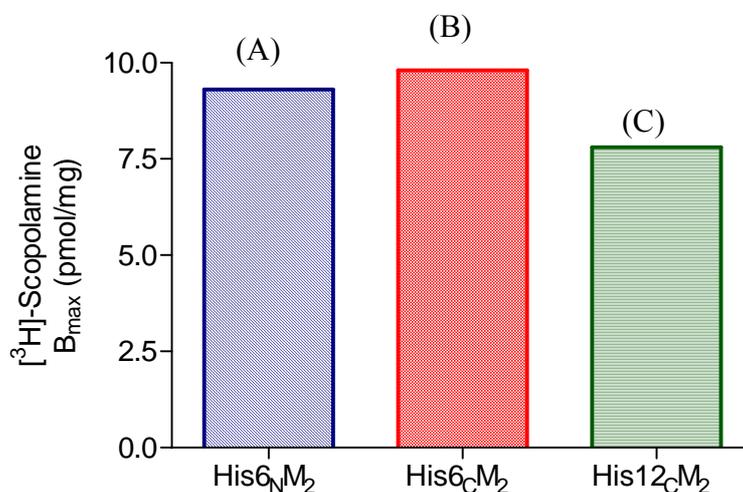
Figure 10. $[^3H]$-Scopolamine binding to Histidine tagged M_2 Muscarinic receptors in membranes prepared from Sf9 cells infected with recombinant baculovirus. B_{max} values were calculated using single site non-linear regression and were 9.3, 9.8 and 7.8 pmol/mg for the $His6_NM_2$, $His6_CM_2$ and $His12_CM_2$, respectively.

Though there are variations in the absolute IC_{50} value between receptor constructs, the rank order potency remains similar (Table 2).

Table 2. Pharmacological profile of M_2R constructs. EC_{50} values are given as determined by a competition assay with $[^3H]$-scopolamine. N/D = Not Determined. Complete competition curves, with replicates, are given in chapter 2 appendix.

	Atropine(nM)	Pirenzepine(μM)	Acetylcholine (μM)
M_2R	26	10	17
$His(6_N)M_2R$	53	3	N/D
$His(6_C)M_2R$	12	1.1	16
$His(12_C)M_2R$	7.3	5.5	20

Whilst the Histidine tagged M_2Rs overall showed lower expression than the un-tagged M_2R, the practical advantage of the Histidine tag in allowing immobilised metal affinity chromatography of the receptors partially offsets the decrease in membrane associated receptor number. Additionally, the expression of the three M_2R constructs meant there was a selection available should optimisation of future steps, such as G-protein coupling and Nickel resin binding, be required.

2.4.3. Expression of the H_1 Histamine Receptor

The $His10_CH_1R$ baculovirus was obtained from Professor Wim deGrip (NCMLS). Similar to the $His6_CM_2R$ baculovirus, integrity of the $His10_CH_1R$ baculovirus and preliminary expression optimisation was confirmed by measurement of $[^3H]$-pyrilamine binding to $Sf9$ cell lysates following viral infection (Figure 11). As has been previously reported, maximum expression of the Histidine tagged H_1R reached maximum levels at 96 hours post infection (Ratnala, et al., 2004). Furthermore, a decrease in $[^3H]$-pyrilamine binding was observed at 120 hours post infection. This is most likely explained by cell lysis and subsequent degradation of protein. The later presence of maximal levels of functional $His10_CH_1R$ is an interesting variation to the pattern observed for the presence of functional $His6_CM_2R$, since both proteins expressed under the same viral promoter and in the same cell line. It may represent a slower maturation rate for the functional $His10_cH_1R$ despite a similar translation rate for the two receptors. Regardless, it highlights the need to optimise the expression conditions for individual proteins/baculoviruses.
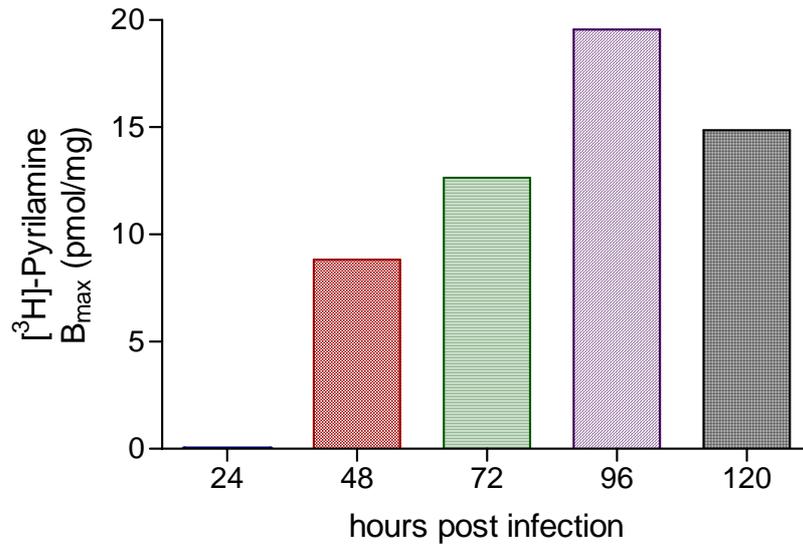
Figure 11. [^{3}H]-pyrilamine binding to cells infected with His10$_c$H$_1$ recombinant baculovirus. Cells were collected at 24 hour intervals post baculovirus addition and assayed for specific [^{3}H]-pyrilamine binding. Non-specific binding was determined in the presence of 10μM triprolidine. B$_{max}$ values were calculated from saturation curves consisting of data points for which the mean ± S.E.M was calculated for three separate experiments.

Urea treated membranes prepared from His10$_C$H$_1$R infected insect cells showed a high level of receptor/ligand ([^{3}H]-pyrilamine) binding, with typical receptor levels in the range of 40-60pmol of specific [^{3}H]-pyrilamine binding per mg of total membrane protein (Figure 12). Although not determined in this study, comparison with previous reports of H$_1$R suggest that addition of the Histidine tag does not effect H$_1$R expression. Leopoldt, et al., (1997) reported an expression level of 1.7pmol/mg, as determined by specific [^{3}H]-pyrilamine binding, for the Guinea Pig H$_1$R in *Sf*9 cells that had been incubated with recombinant baculovirus for 48 hours. This expression level is approximately 30 fold lower than that reported here and elsewhere for the His10$_C$H$_1$R (Ratnala, et al., 2004). The same receptor expressed in CHO cells showed saturable [^{3}H]-pyrilamine binding at 0.5pmol/mg (Fitzsimons, et al., 2004). Thus, for the His10$_c$H$_1$R at least, the *Sf*9/baculovirus protein expression system appears to be the optimal system for expression.
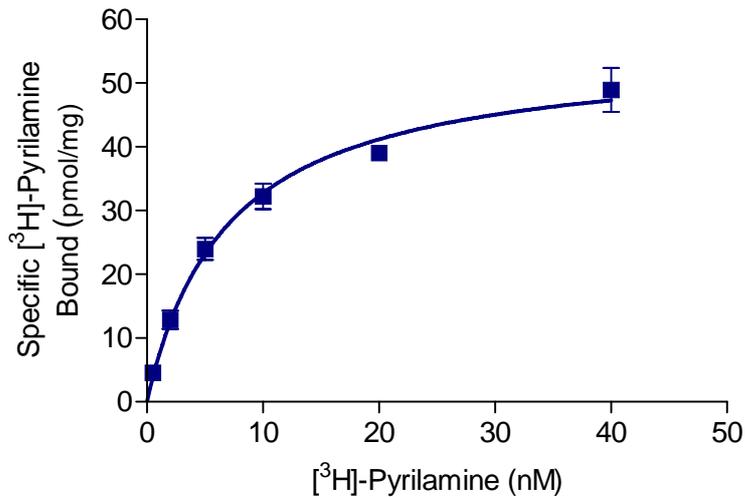
Figure 12. [³H]-Pyilramine binding to urea-treated membranes prepared from *Sf*9 cells infected with recombinant H_1R baculovirus. Analysis revealed a single receptor binding site, saturated at 56pmol/mg of total membrane protein. The radioligand binding site had a K_d of 7nM. Nonspecific binding was determined in the presence of 10μM triprolidine. Data points represent the mean ± S.E.M, n=3.

As expected for the H_1R, the [³H]-pyilramine binding site showed a rank order potency of triprolidine > pyrilamine >> histamine, with EC_{50} values of 1.5nM, 32nM and 70μM for the antagonist, inverse agonist and agonist, respectively (Figure 13) (Ratnala, et al., 2004).
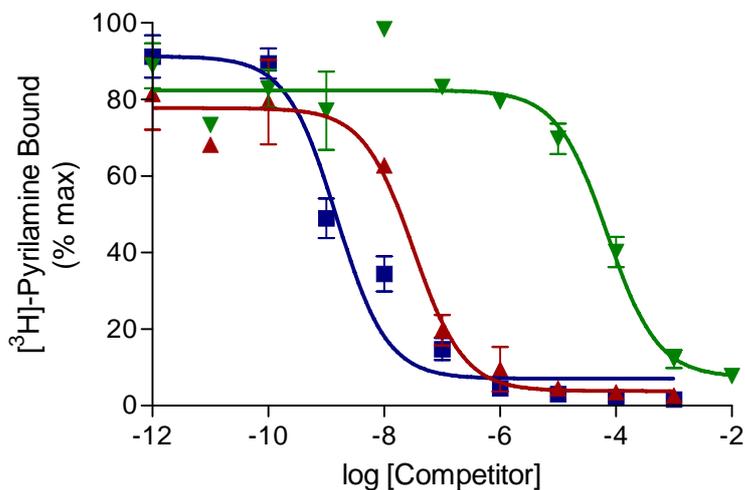
Figure 13. Competition binding for [³H]-pyrilamine binding at the $His10_CH_1$ Receptor. 5nM [³H]-pyrilamine with designated concentrations of triprolidine (blue squares), pyrilamine (red triangles) and histamine (green diamonds). Data points were fitted to a one site sigmoidal dose response from which EC_{50} values were calculated as 1.5nM, 32nM and 70μM for triprolidine, pyrilamine and histamine in that order. Data points represent the mean ± S.E.M, n=3.

2.4.4. Expression of the 5HT$_{2A}$ Serotonin Receptor

Preliminary analysis of 5HT$_{2A}$R expression was carried out on whole cell lysates. Initially, homologous binding assays using the receptor antagonist ketanserin for non-specific binding were performed (due to ligand availability) on cells taken at 24 hour time points following baculovirus infection of *Sf*9 cells. Data from these experiments is shown in Figure 14. High (~50%) non-specific [^{3}H]-ketanserin binding to the cell samples was measured and binding of the radioligand did not saturate (results not shown). High non-specific binding of the radioligand meant the presence or absence of the 5HT$_{2A}$R could not be confirmed at this stage.
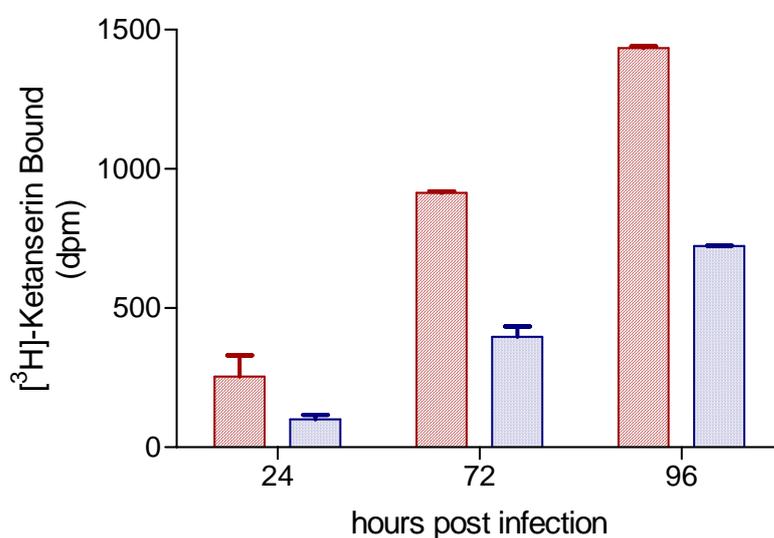

Figure 14. [^{3}H]-Ketanserin binding to 5HT$_{2A}$R baculovirus infected *Sf*9 cells. Total binding is shown by red diagonal lined bars and non-specific binding by blue dotted bars. Non-specific binding was determined in the presence of unlabelled ketanserin (15μM). Each assay contained 50μg of total protein. Results are from a single expression, bars represent assay duplicates.

[^{3}H]-ketanserin binding to urea treated membranes prepared from 5HT$_{2A}$R baculovirus infected *Sf*9 cells gave similar results (Figure 15). Non-specific binding of [^{3}H]-ketanserin to the membranes was, in the presence of unlabelled ketanserin (20μM), ~ 50% of total binding. Radioligand binding did not saturate even though at the protein concentration used in the assay total binding of the [^{3}H]-ketanserin was ≤ 10% of free [^{3}H]-ketanserin.
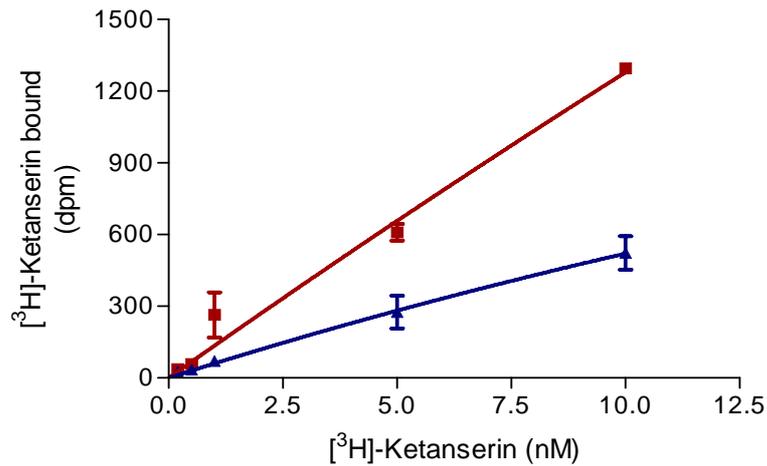
Figure 15. [3H]-Ketanserin binding to urea-treated membranes prepared from 5HT$_{2A}$R baculovirus infected *Sf*9 cells. Total binding is shown by red squares and non-specific binding by blue triangles. Non-specific binding was determined in the presence of unlabelled ketanserin (20μM). Each assay contained 50μg of total protein. Results are from a single expression, error is calculated from assay triplicates. Each point represents the mean ± S.E.M., n = 3. At a volume equal to that used in the assay, 5nM [3H]-Ketanserin produces ~25000dpm.

In addition to ketanserin, both clozapine and mianserin were used in an effort to block non-specific [3H]-ketanserin binding. Both ligands have nanomolar affinity for the 5HT$_{2A}$R (Peroutka and Snyder, 1981; Seeman, et al., 1997). The use of clozapine decreased non-specific binding of [3H]-ketanserin to 5HT$_{2A}$R baculovirus infected *Sf*9 cell lysates to 20 – 35% of total radioligand but the binding did not saturate even at 50nM of [3H]-ketanserin and with a total protein concentration in the assay such that bound radioligand was ≤ 10% of free radioligand (Figure 16).
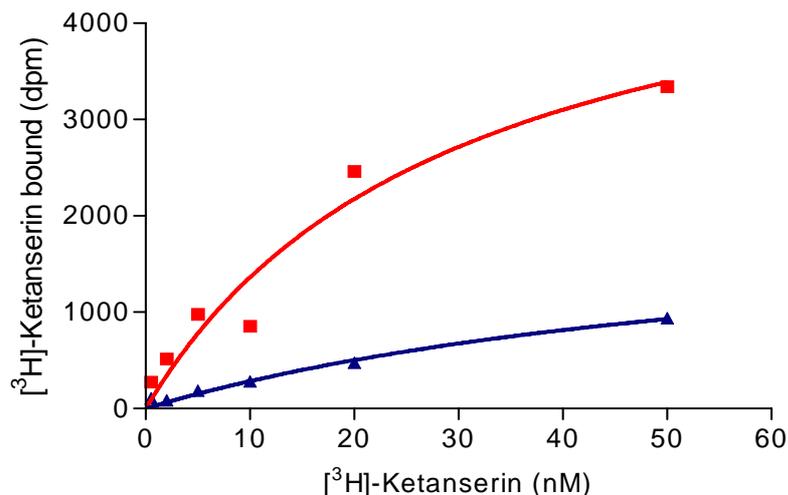
Figure 16. [3H]-Ketanserin binding to whole cell lysates prepared from 5HT$_{2A}$R infected cells. Total binding is shown by red squares, binding of the radioligand in the presence of 15μM clozapine is shown by blue triangles. Each assay contained 25μg of total protein. Each point represents a single experiment. At a volume equal to that used in the assay, 5nM [3H]-Ketanserin produces ~12000dpm.

The binding of [3H]-ketanserin at a concentration of 20 – 50nM may be an artifact of the high free radioligand concentration. If these points are removed from the data a potential saturation curve for the [3H]-ketanserin is generated (Figure 17).
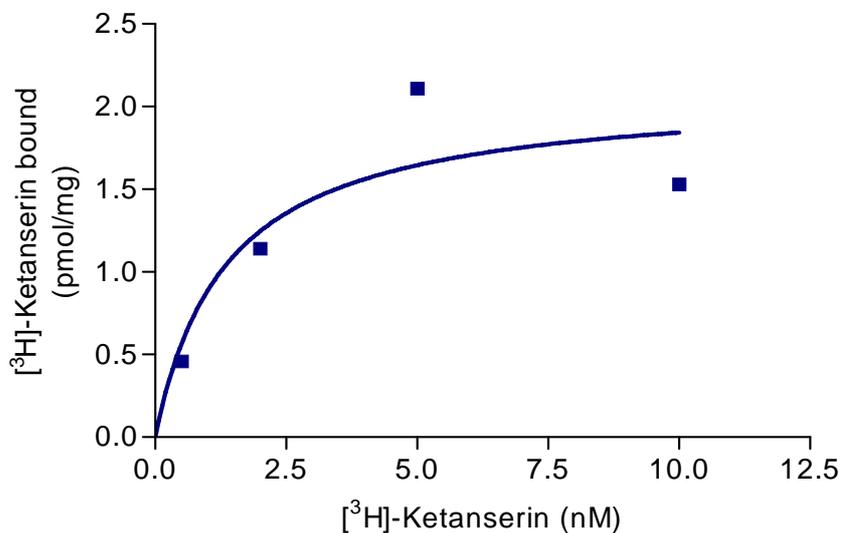

Figure 17. [3H]-Ketanserin binding whole cell lysates prepared from 5HT$_{2A}$R infected cells. Non-specific binding of the radioligand was ~30%. Data points are from a single experiment. Data was fitted to a one site binding hyperbola.

Though the data can be fitted to a saturation curve, non-specific binding is discouragingly high. High non-specific binding of [3H]-ketanserin was also observed when the same experiment was performed on urea-treated *Sf*9 membranes, or in the presence of the serotonin receptor antagonist mianserin (30 – 60% non-specific radioligand, results not shown). Thus the expression of the 5HT$_{2A}$R in the baculovirus infected *Sf*9 cells could not be conclusively confirmed. The results presented in Figures 14, 15 and 16 do more to suggest the absence of the 5HT$_{2A}$R. In addition to the results presented here, a His6$_C$5HT$_{2A}$R baculovirus was independently produced by Dr Janelle Williams (CSIRO). Cells collected following infection with the His6$_C$5HT$_{2A}$R baculovirus did not show saturable [3H]-ketanserin binding and non-specific binding in the presence of clozapine (10μM) was >60% (results not shown). Taken together, these results suggest that the 5HT$_{2A}$R is not being functionally expressed by the baculovirus infected *Sf*9 cells, despite the virus containing the receptor gene and being infective (Figure 6). 5HT$_{2A}$R expression using HEK-293 cells (Knight, et al., 2004) and rat cells (Garnovskaya, et al., 1995) has been reported but there do not appear to be reports of 5HT$_{2A}$R expression using the baculovirus/insect cell system. The 5HT$_{4A}$R has been expressed using recombinant baculovirus infection of *Sf*9 cells, though pmol/mg values were not reported (Ponimaskin,

et al., 2001). The rat $5HT_{2C}R$ was expressed in *Sf9* cells to levels of several hundred thousand receptors per cell as determined by $[^3H]$-mesulergine binding (Labrecque, et al., 1995). Whilst $5HT_{2A}R$ has not been expressed using baculovirus infection of insect cells, the receptor has been stably expressed in *Sf9* cells for functional studies (Harvey, et al., 2003). The difficulties experienced in unequivocally expressing the $5HT_{2A}R$, successful expression of other receptors and time limitations meant that this receptor was not utilised for the remainder of the study. If expression of the $5HT_{2A}R$ is required for future studies a different expression such as mammalian cell culture may be required.

Both the time course and level of expression varied substantially between the muscarinic, histamine and serotonin receptors studied. This is not overly surprising since despite being from the same family, the receptors share little sequence homology. Alignment of the amino acid sequences, using the local similarity program, SIM (http://ca.expasy.org/tools/sim-prot.html), shows an overall sequence homology of 28.7%, 32% and 32.6% for comparison of H_1R/M_2, $5HT_{2A}R/M_2$ and $5HT_{2A}R/H_1R$, respectively. The variability in the amino acid sequence (and thus ultimately the gene sequence) may account for the variability in protein production if the insect cell is less abundant in particular factors required for translation (e.g. particular tRNAs). As a class, the 7TMRs show low expression compared to soluble proteins expressed using the baculovirus/insect cell system. Under control of the same viral polyhedrin promoter intracellular proteins, such as the G-proteins, are readily expressed at up to 150 mg per Litre (at 2×10^6 cells per Litre) quantities (Graber, et al., 1994) whereas expression levels reported here (10-60pmol/mg; 0.3 – 2mg per Litre, for a 53kDa protein) are around 100 fold lower than this but are standard for 7TMRs. The lower expression levels of membrane proteins is likely due to the need for the cell to be both effective and highly efficient in protein translocation and folding. The availability of suitable chaperones and the extent of stress placed on the endoplasmic reticulum may also be contributing factors in lower levels of membrane protein expression.

2.4.5. Ligand Culture

Given the knowledge that membrane associated receptor levels are related to receptor exposure to ligands, it was hypothesised that exposure of baculovirus infected insect cells to ligands associated with the receptor being expressed may be a simple method to increase membrane associated receptor number. For the $His6_CM_2R$, expression is at near maximum

at 48 hours post infection (Figure 7), addition of a drug at this time point; where receptor expression is near maximal but cells remain viable (approximately 98% viable by Trypan blue staining, not shown), may result in changes in the receptor trafficking and/or expression. This theory was also tested on the $His10_CH_1R$ (however ligands were added at 72 hours post infection) and the $His6_CD_{2L}R$. The dopamine receptor virus was a gift from Dr Janelle Williams (CSIRO). Ligand culture experiments (using all of the ligands mentioned) with the $His6_CM_2R$ and the $His10_CH_1R$ were repeated three times while for the $His6_CD_{2L}R$ duplicate experiments were used. The following results are representative of one cell culture experiment. Trends in expression level variation for the ligand set were consistent but, as with all cell culture work, there were variations in the starting (untreated control) expression levels.

24 hour exposure of $His6_CM_2R$ baculovirus infected insect cell culture to atropine resulted in a 2 fold increase in membrane associated [^{3}H]-scopolamine binding (compare Figure 18B and 18A). As an inverse agonist/antagonist, atropine is expected to increase cell membrane associated receptor expression (Milligan and Bond, 1997). In a similar experiment, May, et al., (2005) reported a 1.4 fold increase in cell membrane associated M_2R expression in recombinant CHO cells treated with atropine, as determined by specific [^{3}H]-scopolamine binding on intact cells.
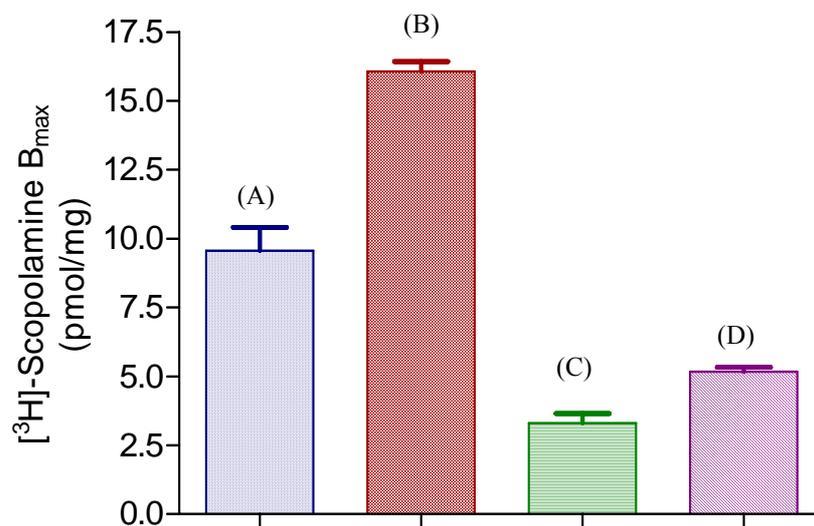

Figure 18. [^{3}H]-Scopolamine binding to $His6_CM_2R$ urea-treated membranes prepared from ligand treated, infected *Sf*9 cells. (A) No ligand treatment, $B_{max} \sim 8.4$pmol/mg. (B) Treatment with atropine, $B_{max} \sim 15.8$pmol/mg. (C)Treatment with acetylcholine, $B_{max} \sim 3.3$pmol/mg. (D) Treatment with pirenzepine, $B_{max} \sim 5.5$pmol/mg. Results are representative of one of three complete culture experiments. Replicates represent assay points from a single membrane preparation, mean ± S.E.M., n = 3.

Interestingly, cells cultured with pirenzepine, a M_2R inverse agonist, showed a 1.5 fold decrease in membrane associated receptor expression compared to the untreated control (compare Figure 18D and 18A). This is in contrast to experiments performed in CHO-K1 cells expressing either a wild type or N410Y M_2R mutant (Nelson, et al., 2006). This is likely due to variation in pirenzepine concentrations used – 50nM in this study and 100μM with CHO cells, particularly as the ligand treatment would be expected to elicit dose dependant effects (Nelson, et al., 2006). $His6_CM_2R$ baculovirus infected $Sf9$ cells cultured with acetylcholine showed a 2.4 fold decrease in membrane associated receptor expression, as determined by specific [^{3}H]-scopolamine binding, compared to cells cultured without the drug (compare Figure 18C and 18A). This compares well with the effect of carbachol addition to CHO cells expressing the M_2R where, following agonist addition, a decrease in membrane associated receptor number was observed (May, et al., 2005; Nelson, et al., 2006). Thus levels of membrane associated $His6_CM_2R$ expression as a result of these treatments can be summarised; atropine cultured >> untreated > pirenzepine cultured > acetylcholine cultured, in decreasing order of specific [^{3}H]-scopolamine binding level.

To determine if receptor expression levels could be increased, ligand culture experiments were also trialed with $His10_CH_1R$ expressing $Sf9$ cells (Figure 19).
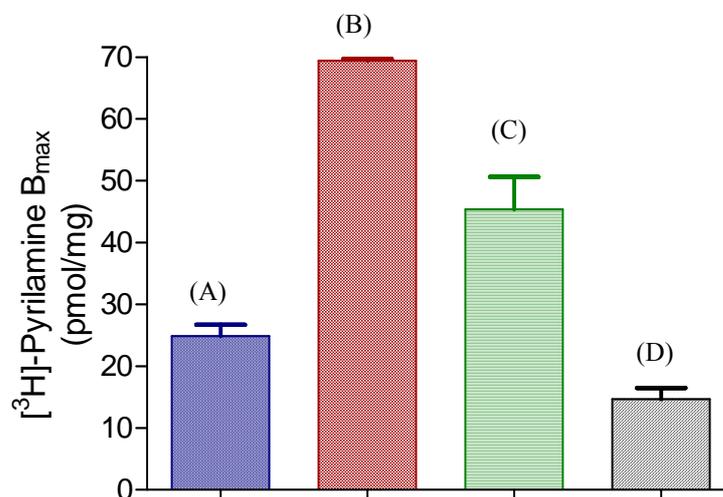

Figure 19. [^{3}H]-pyrilamine binding to $His10_CH_1R$ urea-treated membranes prepared from ligand treated, infected $Sf9$ cells. (A) No ligand treatment, B_{max} ~ 25pmol/mg. (B) Treatment with triprolidine, B_{max} ~ 69pmol/mg. (C)Treatment with pyrilamine, B_{max} ~ 45pmol/mg. (D) Treatment with histamine, B_{max} ~ 14pmol/mg. Results are representative of one of two complete culture experiments. Replicates represent assay points from a single membrane preparation, mean ± S.E.M., n = 3.

Treatment of $His10_CH_1R$ baculovirus infected $Sf9$ cells with the H_1R inverse agonist triprolidine (Figure 19B), resulted in a 2.7 fold increase in receptor number in the final

membrane preparation, compared to membranes from untreated cells (Figure 19A). This was comparable to results reported for the treatment of the H_2 histamine receptor expressing CHO cells with cimetidine (also a histamine receptor inverse agonist) (Smit, et al., 1996). Another inverse agonist, pyrilamine, also increased membrane associated receptor density by 1.8 fold (compare Figure 19C and 19A). Treatment with the agonist histamine decreased [^{3}H]-pyrilamine binding sites in the final membrane preparation by 1.6 fold compared to the control (compare Figure 19D and 19A). This compared well to results published for membrane associated H_1R and, separately, H_2R in CHO cells treated with 100μM Histamine for 24 hours (Miyoshi, et al., 2006; Smit, et al., 1996). As for the His6$_C$M$_2$R experiments, treatment of His10$_C$H$_1$R expressing *Sf*9 cells with a high affinity (nM) inverse agonist (triprolidine) gave the greatest increase in receptor density compared to other treatments.

As a final assessment of the viability of ligand culture on receptor expression, a ligand culture experiment was carried out on *Sf*9 cells expressing the D_{2L} dopamine receptor (D_{2L}R, Figure 20).
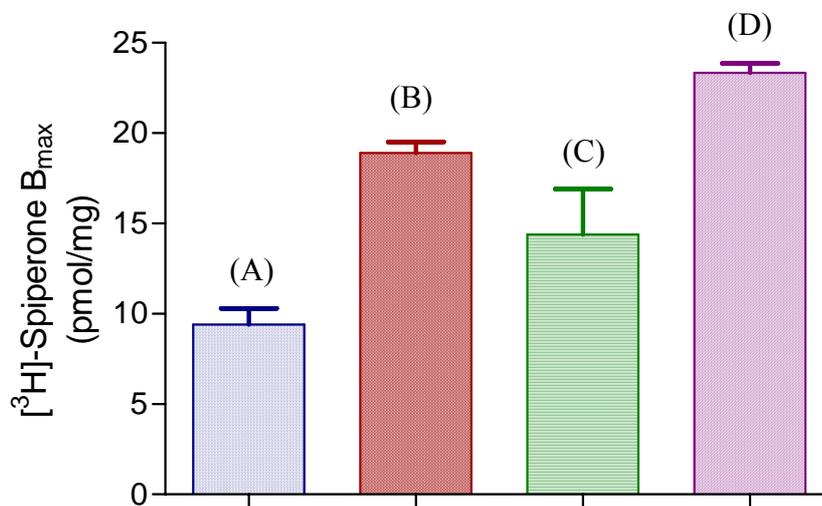

Figure 20. [^{3}H]-spiperone binding to His6$_C$D$_{2L}$R membranes prepared from ligand treated, infected *Sf*9 cells. (A) No ligand treatment, $B_{max} \sim$ 9.2pmol/mg. (B) Treatment with bromocryptine, $B_{max} \sim$ 19.1pmol/mg. (C) Treatment with haloperidol, $B_{max} \sim$ 11.3pmol/mg. (D) Treatment with NPA, $B_{max} \sim$ 23.2pmol/mg. Results are representative of one of two complete culture experiments. Replicates represent assay points from a single membrane preparation, mean ± S.E.M., n = 3.

Addition of dopamine receptor specific ligands to the His6$_C$D$_{2L}$R infected culture produced interesting results (Figure 20). In contrast to effects seen with agonist treated His6$_C$M$_2$R and His10$_C$H$_1$R expressing *Sf*9 cells, a 2 fold increase in membrane associated receptor

was observed following treatment of His6$_C$D$_{2L}$R baculovirus infected *Sf*9s with either of the dopamine agonists, norapomorphine (NPA) or bromocryptine. Increases in membrane associated D$_{2L}$R have been observed with dopamine (10µM) treatment of both baculovirus infected *Sf*9 cells and yeast cells (Grunewald, et al., 2004; Ng, et al., 1997). Additionally, both yeast and C$_6$ glioma cells have demonstrated an increase in receptor number per cell, for cells treated with NPA (De Lean, et al., 1980; Grunewald, et al., 2004). 24 hour treatment with the inverse agonist haloperidol also increased (1.2 fold, compare Figure 20C and 20A) [^{3}H]-spiperone binding sites on the *Sf*9 membranes but to a lesser extent than dopamine or NPA.

Several experiments would be required to further characterise the effect of ligand addition to the infected cell cultures, including a time course of receptor expression after ligand addition and ligand dose dependence of expression variation. The results presented here support and extend observations of ligand modulated changes in membrane associated receptor number of the M$_2$R, H$_1$R and D$_2$R (Grunewald, et al., 2004; May, et al., 2005; Smit, et al., 1996). Ligand addition to infected *Sf*9 cultures produced significant variations in membrane associated receptor number for the three receptors used in this study. There are several possible (and perhaps not individual) explanations for the ligand induced change in membrane associated receptor number: 1) Ligands are modulating at the mRNA level. This does not appear to be the case for the D$_{2L}$R, where published work has shown that co-treatment of receptor expressing cells with agonist and cycloheximide (which inhibits translational elongation and thus protein synthesis) had no significant effect on the increase in membrane associated receptor (Ng, et al., 1997; Starr, et al., 1995). mRNA mediated changes have not however been ruled out as possibilities to explain ligand induced changes in M$_2$ and H$_1$R expression. 2) Existing pools of receptor are being relocated between the outer cell membrane and inner cell compartments. This phenomonen has best been demonstrated in dopamine treated, D$_{2L}$R expressing *Sf*9 cells (Ng, et al., 1997). Mutant H$_1$R lacking phosphorylation sites are not down-regulated by histamine, suggesting that decrease in membrane associated receptor is by trafficking from the surface of the cell (Miyoshi, et al., 2006). This hypothesis may not be entirely applicable in this study however, as intracellular membranes should also be represented in the membrane fraction used in ligand binding assays. 3) Ligand bound receptors are being protected from (agonist independent) degradation. This is a common hypothesis for all type A 7TMRs (Grunewald, et al., 2004; Milligan and Bond, 1997; Nelson, et al., 2006). It is well

supported by the observation that high affinity ligands lead to an increase in receptor number (Figure 18, 19 and 20). 4) The ligands may be stabilising receptors during folding, so there are more correctly folded receptors available for export to the external membrane. This of course should only be true for membrane permeable ligands, a property which is difficult to determine (Alper, 2002). Explanation of receptor trafficking in the presence of receptor specific ligands was not the purpose of this study. The aim was to identify a simple method for increasing receptor number in the $Sf9$ cell membrane. To this extent the ligand culture experiments achieved their aim, with several ligands identified to increase receptor density in the membrane. Future work with the M_2Rs and the $His10_CH_1R$ used atropine (50nM) and triprolidine (50nM) addition to infected $Sf9$ cell cultures at 48/72 hours post infection. Whilst agonist treatment of $His6_CD_{2L}R$ expressing cells increased expression levels, the price of the drugs would make their large scale use a costly exercise.

2.5. Conclusions

Recombinant baculoviruses were produced for a 6xHis, N terminal tagged M_2 muscarinic receptor and for 6xHis and 12xHis C terminal tagged M_2 muscarinic receptors. The baculovirus/Sf9 cell system was used to express six receptors – the M_2R, $His6_NM_2R$, $His6_CM_2R$, $His12_CM_2R$, $His10_CH_1R$ and the $5HT_{2A}R$. Expression levels were determined on urea treated membranes prepared from recombinant bavulovirus infected Sf9 cells. Un-tagged M_2R expressed at $15 - 20$ pmol/mg of total membrane protein, Histidine tagging of the receptor decreased expression levels to around $10 - 15$ pmol/mg regardless of position or length of tag. The $His10_CH_1R$ expressed at between $40 - 60$pmol/mg of total membrane protein. Both the M_2R and H_1R binding sites were confirmed by competition binding assays using known receptor ligands. Preliminary results suggested that the $5HT_{2A}R$ can not be functionally expressed using the baculovirus/Sf9 expression system.

Membrane associated receptor was manipulated by addition of receptor specific ligands to infected insect cell cultures. Addition of the muscarinic receptor antagonist atropine to $His6_CM_2R$ expressing Sf9 cells increased receptor density in the membrane by 2 fold compared to receptor expression in untreated controls. $His10_CH_1R$ density in the membrane was increased by 2.7 fold compared to untreated Sf9 cells, when the antagonist triprolidine was added to the infected cell cultures.